

Genome-Wide Analysis of the RNA-DEPENDENT RNA POLYMERASE6/DICER-LIKE4 Pathway in *Arabidopsis* Reveals Dependency on miRNA- and tasiRNA-Directed Targeting

Miya D. Howell,^a Noah Fahlgren,^b Elisabeth J. Chapman,^b Jason S. Cumbie,^a Christopher M. Sullivan,^a Scott A. Givan,^a Kristin D. Kasschau,^a and James C. Carrington¹

^aCenter for Genome Research and Biocomputing, Department of Botany and Plant Pathology, Oregon State University, Corvallis, Oregon 97331

^bMolecular and Cellular Biology Graduate Program, Oregon State University, Corvallis, Oregon 97331

Posttranscriptional RNA silencing of many endogenous transcripts, viruses, and transgenes involves the RNA-DEPENDENT RNA POLYMERASE6/DICER-LIKE4 (RDR6/DCL4)-dependent short interfering RNA (siRNA) biogenesis pathway. *Arabidopsis thaliana* contains several families of *trans*-acting siRNAs (tasiRNAs) that form in 21-nucleotide phased arrays through the RDR6/DCL4-dependent pathway and that negatively regulate target transcripts. Using deep sequencing technology and computational approaches, the phasing patterns of known tasiRNAs and tasiRNA-like loci from across the *Arabidopsis* genome were analyzed in wild-type plants and silencing-defective mutants. Several gene transcripts were found to be routed through the RDR6/DCL4-dependent pathway after initial targeting by one or multiple miRNAs or tasiRNAs, the most conspicuous example of which was an expanding clade of genes encoding pentatricopeptide repeat (PPR) proteins. Interestingly, phylogenetic analysis using *Populus trichocarpa* revealed evidence for small RNA-mediated regulatory mechanisms within a similarly expanded group of PPR genes. We suggest that posttranscriptional silencing mechanisms operate on an evolutionary scale to buffer the effects of rapidly expanding gene families.

INTRODUCTION

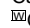
RNA-based silencing in eukaryotes is involved in inactivation or repression of a variety of endogenous and exogenous genetic elements, including genes, transposons and retroelements, viruses, and transgenes (Baulcombe, 2004; Mello and Conte, 2004; Martienssen et al., 2005). The core silencing mechanism involves a double-stranded RNA (dsRNA) trigger formed by any of several mechanisms, including bidirectional transcription of DNA, self-complementary RNA foldbacks, or RNA-dependent RNA transcription. In canonical RNA silencing, small RNAs of ~21 to 24 nucleotides in either of two biogenesis classes—short interfering RNA (siRNA) from perfectly complementary dsRNA or microRNA (miRNA) from imperfect foldbacks—are formed, although recently discovered classes of small RNAs (PIWI-interacting RNAs and 21U-RNAs) with novel characteristics and biogenesis mechanisms have been identified (Aravin et al., 2006; Girard et al., 2006; Grivna et al., 2006a, 2006b; Kim, 2006; Lau et al., 2006; Ruby et al., 2006). siRNAs and miRNAs arise by the activities of RNase III-type activities of DICER or DICER-LIKE

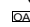
(DCL) enzymes in complexes that catalyze formation of small RNA duplexes (Henderson et al., 2006; Vazquez, 2006). Generally, one strand of the duplex is incorporated into RNase H-like ARGONAUTE (AGO)-containing effector complex, conferring sequence-specific guide functions to the AGO protein (Tomari and Zamore, 2005; Tolia and Joshua-Tor, 2007).

Plants evolved several classes of siRNAs that form by distinct mechanisms and function in separate effector pathways (Brodersen and Voinnet, 2006; Vaucheret, 2006). The most abundant siRNA class (24 nucleotides) arises by RNA-DEPENDENT RNA POLYMERASE2 (RDR2)/DCL3/PolIV activities and functions through AGO4 to initiate or maintain transcriptional silencing through DNA methylation and histone modifications (Zilberman et al., 2003, 2004; Chan et al., 2004; Xie et al., 2004; Herr et al., 2005; Kanno et al., 2005; Onodera et al., 2005; Pontier et al., 2005; Tran et al., 2005). This pathway is associated with transposons, retroelements, and other repeat classes (Xie et al., 2004; Lu et al., 2006; Rajagopalan et al., 2006; Kasschau et al., 2007). Other siRNA classes function at the posttranscriptional level. Silencing of viral RNA and transgene transcripts involves RDR6/DCL4-dependent siRNAs (21 nucleotides) and, for at least some viruses, DCL2-dependent siRNAs (22 nucleotides) (Waterhouse et al., 2001; Xie et al., 2004; Bouche et al., 2006; Deleris et al., 2006; Fusaro et al., 2006; Waterhouse and Fusaro, 2006; Mourrain et al., 2007). Dual siRNA biogenesis pathways may be an important adaptation during antiviral defense due to the ability of viruses to suppress individual pathways (Deleris et al., 2006). The RDR6/DCL4 pathway also catalyzes formation of *trans*-acting siRNAs (tasiRNAs), which are endogenous regulators of several mRNAs, as discussed

¹To whom correspondence should be addressed. E-mail carrington@cgrb.oregonstate.edu; fax 541-737-3045.

The author responsible for distribution of materials integral to the findings presented in this article in accordance with the policy described in the Instructions for Authors (www.plantcell.org) is: James C. Carrington (carrington@cgrb.oregonstate.edu).

 Online version contains Web-only data.

 Open Access articles can be viewed online without a subscription. www.plantcell.org/cgi/doi/10.1105/tpc.107.050062

below (Peragine et al., 2004; Vazquez et al., 2004b; Allen et al., 2005; Gascioli et al., 2005; Xie et al., 2005; Yoshikawa et al., 2005). In addition, natural antisense transcript-derived siRNAs are formed through induced, bidirectionally oriented transcript pairs, but through biogenesis mechanisms that are not yet clear (Borsani et al., 2005; Wang et al., 2005; Katiyar-Agarwal et al., 2006; Munroe and Zhu, 2006).

The tasiRNAs form through a mechanism that yields 21-nucleotide, phased siRNAs from *TAS* transcripts that are initially processed by miRNA-guided cleavage (reviewed in Vaucheret, 2005; Willmann and Poethig, 2005). Specifically, miR173 (*TAS1* and *TAS2*), miR390 (*TAS3*), and miR828 (*TAS4*) function as processing guides on primary transcripts to yield defined 5' or 3' ends on precursor RNAs, respectively (Allen et al., 2005; Yoshikawa et al., 2005; Rajagopalan et al., 2006). SUPPRESSOR OF GENE SILENCING3 (*SGS3*) may stabilize the precursor after miRNA-guided cleavage and facilitate dsRNA formation catalyzed by RDR6 (Mourrain et al., 2000; Yoshikawa et al., 2005). The dsRNA precursor is then processed in an end-dependent manner by DCL4, which yields duplexes containing 21-nucleotide siRNAs with 2-nucleotide overhangs at each 3' end (Dunoyer et al., 2005; Gascioli et al., 2005; Xie et al., 2005). Functional tasiRNAs with complementarity to target transcripts arise from multiple processing cycle positions, depending on the locus (Vazquez et al., 2004b; Allen et al., 2005; Yoshikawa et al., 2005).

Biological functions have been assigned to the *TAS3* family tasiRNAs, which downregulate mRNAs encoding several AUXIN RESPONSE FACTORS, including *ARF3* (*ETTIN*) and *ARF4* (Allen et al., 2005; Williams et al., 2005). *TAS3*-mediated regulation of *ARF3* and *ARF4* mRNAs is required for proper timing of vegetative shoot development and establishment of leaf polarity (Adenot et al., 2006; Fahlgren et al., 2006; Garcia et al., 2006; Hunter et al., 2006). Formation, stability, or activity of *TAS3* tasiRNAs requires AGO7 (*ZIPPY*), which was originally identified genetically due to its role in vegetative phase change (Hunter et al., 2003; Adenot et al., 2006; Fahlgren et al., 2006). miR390-guided *TAS3*-like loci evolved in ancient land plants as revealed by comparative phylogenetic analyses (Allen et al., 2005; Axtell et al., 2006; Talmor-Neiman et al., 2006). Biological functions for the nonconserved *TAS1* and *TAS2* tasiRNAs are not yet clear. These tasiRNAs target mRNAs encoding several members of the pentatricopeptide repeat protein (*PPR*) family as well as mRNAs encoding proteins of unknown function (Peragine et al., 2004; Vazquez et al., 2004b; Allen et al., 2005; Yoshikawa et al., 2005).

In this article, the phasing patterns of tasiRNAs identified from sequenced libraries were analyzed. These libraries were generated by highly parallel sequencing methods using wild-type plants and RNA silencing-defective mutants (Fahlgren et al., 2006; Kasschau et al., 2007; <http://asrp.cgrb.oregonstate.edu/db/>). Genome-wide scans for small RNAs resembling tasiRNAs revealed several new RDR6-dependent loci that yield phased siRNAs. Many of these loci correspond to protein-coding genes, including many members of the large *PPR* family, with transcripts targeted by miRNAs and other tasiRNAs.

RESULTS

Analysis of *TAS1*, *TAS2*, and *TAS3* Families

A detailed analysis of small RNAs from known *TAS* loci was done using populations of sequenced small RNAs from wild-type (*Col-0*), *dcl* mutant (*dcl1-7*, *dcl2-1*, *dcl3-1*, and *dcl4-2*), and *rdr* mutant (*rdr1-1*, *rdr2-1*, and *rdr6-15*) plants (Fahlgren et al., 2007; Kasschau et al., 2007; <http://asrp.cgrb.oregonstate.edu/db/>). tasiRNAs from *TAS1*, *TAS2*, and *TAS3* families were represented by at least 836 reads (Table 1), and all were RDR6 dependent (Table 2). Only two reads were obtained for the *TAS4* locus. Small RNAs from *TAS* loci were predominantly 21 nucleotides in length, and this size class was greatly reduced in the *dcl4-2* mutant (all values normalized for sequence population size; Table 2). Additionally and as shown previously, tasiRNAs in these sequenced populations were dependent on DCL1 (see Supplemental Table 1 online; Kasschau et al., 2007).

The fact that validated tasiRNAs, or tasiRNAs with high-quality predicted targets, arise from the *TAS* locus positions residing up to 12 processing cycles away from the initiation cleavage sites (Figure 1) points to the importance of accurate phasing to generate small RNAs with sufficient complementarity to target sequences. Therefore, the phasing patterns of small RNAs from the miR173-guided cleavage site (*TAS1* and *TAS2* loci) and 3' miR390-guided cleavage site (*TAS3* loci) were analyzed. Small RNA sequence data from wild-type and *rdr2-1* mutant (no effect on tasiRNA biogenesis) plants were used to develop an algorithm that converted phase position and amplitude (small RNA abundance) data into phase signals. First, a sense-antisense small RNA consolidation step was developed to unify sequence data from both strands. Small RNA pairs from sense-antisense positions

Table 1. *Arabidopsis TAS* Families

<i>TAS</i> Family ^a	No. Loci/Family	Conserved ^b	No. Reads ^c	Target Family	Target Function	Target Validation ^d
<i>TAS1</i>	3	N	1739	Unclassified	Unknown	Y
				<i>PPR</i>	RNA binding	Y
<i>TAS2</i>	1	N	3570	<i>PPR</i>	RNA binding	Y
<i>TAS3</i>	3	Y	836	<i>ARF</i>	Transcription factor	Y
<i>TAS4</i>	1	NC	2	<i>MYB</i>	Transcription factor	Y

^aPeragine et al. (2004), Vazquez et al. (2004b), Allen et al. (2005), and Rajagopalan et al. (2006).

^bConserved between *Arabidopsis* and *Populus*. NC, not clear (Rajagopalan et al., 2006).

^cTotal reads from each *TAS* locus from all libraries in the ASRP database (<http://asrp.cgrb.oregonstate.edu/db/>).

^dReviewed by Vaucheret (2006).

Table 2. *Arabidopsis* Phased Small RNA-Generating Loci

		21-nt Small RNA Reads ^a		21-nt/Non-21-nt Small RNA ^a		miRNA Phase Initiator ^b	miRNA-Initiated Phasing (Peak P Score) ^c	tasiRNA Phase Initiator ^b	tasiRNA-Initiated Phasing (Peak P Score) ^c
Gene	Gene/Gene Family	Col-0 and <i>rdr2</i>	<i>rdr6</i>	Col-0	<i>dcl4</i>				
tasiRNA loci									
At2g27400	<i>TAS1a</i>	384	0	347/60	1/7	miR173	Y (33.1)		
At1g50055	<i>TAS1b</i>	217	0	176/17	6/18	miR173	Y (25.4)		
At2g39675	<i>TAS1c</i>	377	0	333/99	2/23	miR173	Y (22.2)		
At2g39681	<i>TAS2</i>	855	0	698/192	18/98	miR173	Y (31.8)		
At3g17185	<i>TAS3a</i>	380	0	283/78	31/23	5' miR390	N	<i>TAS3a</i> 3'D2(–)	Y (3.25)
						3' miR390	Y (7.7)		
At5g49615	<i>TAS3b</i>	36	0	14/4	1/8	5' miR390	N		
						3' miR390	Y (2.2)		
Other phased small RNA-generating loci									
At1g62910	<i>PPR</i>	290	0	243/65	0/1	5' miR161.1	Y (7.4)	5' TAS2 3'D6(–)	Y (18.2)
						5' miR161.2	Y (2.2)	5' TAS2 3'D11(–)	N
						5' miR400	N		
						3' miR161.1	Y (2.3)	3' TAS2 3'D6(–)	Y (5.3)
						3' miR161.2	Y (1.8)	3' TAS2 3'D11(–)	N
						3' miR400	N		
At1g63130	<i>PPR</i>	231	0	201/45	0/1	miR161.1	Y (7.7)	TAS2 3'D6(–)	Y (17.7)
						miR161.2	Y (4.8)	TAS2 3'D9(–)	N
						miR400	N	TAS2 3'D11(–)	N
At1g62930	<i>PPR</i>	153	0	125/40	0/1	miR161.1	Y (2.0)	<i>TAS1a</i> 3'D9(–)	N
						miR161.2	Y (5.5)	TAS2 3'D11(–)	N
						miR400	N		
At1g63080	<i>PPR</i>	138	0	125/30	0/0	miR161.1	Y (2.3)	TAS2 3'D6(–)	Y (9.9)
						miR161.2	Y (2.2)	TAS2 3'D9(–)	N
						miR400	N	TAS2 3'D11(–)	N
At1g63400	<i>PPR</i>	87	0	74/26	0/1	miR161.1	Y (1.9)	TAS2 3'D6(–)	N
						miR161.2	N	TAS2 3'D11(–)	N
						miR400	N		
At1g63150	<i>PPR</i>	96	0	76/15	0/0	miR161.1	N	TAS2 3'D6(–)	Y (17.2)
						miR161.2	Y (5.8)	TAS2 3'D11(–)	N
						miR400	N		
At1g63070	<i>PPR</i>	68	0	55/12	0/0	miR161.2	N	TAS2 3'D6(–)	Y (9.9)
						miR400	N	TAS2 3'D9(–)	N
								TAS2 3'D11(–)	N
At1g63330	<i>PPR</i>	37	0	31/16	0/0	miR161.2	N	TAS2 3'D6(–)	N
						miR400	N	<i>TAS1a</i> 3'D9(–)	N
								TAS2 3'D11(–)	N
At1g62590	<i>PPR</i>	33	0	26/10	0/0	miR161.2	N	TAS2 3'D6(–)	Y (2.6)
						miR400	N	<i>TAS1a</i> 3'D9(–)	N
								TAS2 3'D11(–)	N
At5g38850	TIR-NBS-LRR	81	0	75/11	0/1	NI ^d	N (4.4)		
At1g12820	<i>AFB3</i>	10	0	7/0	0/1	miR393	Y (1.4) ^e		
At5g41610	<i>ATCHX18</i>	23	0	6/4	1/3	miR856	Y (1.6)		
						miR780	N		

^aRaw small RNA reads were not normalized for repeats or library size. nt, nucleotide.^bmiRNAs or tasiRNAs that were experimentally validated to guide cleavage of the target are indicated in bold.^cY indicates that at least three small RNAs within eight 21-nucleotide cycles are in phase with the target site. The peak score is based on 20- to 25-nucleotide total small RNA reads from Col-0 and *rdr2-1* libraries.^dNI, not identified.^ePhasing is one nucleotide offset from the miR393-guided cleavage site.

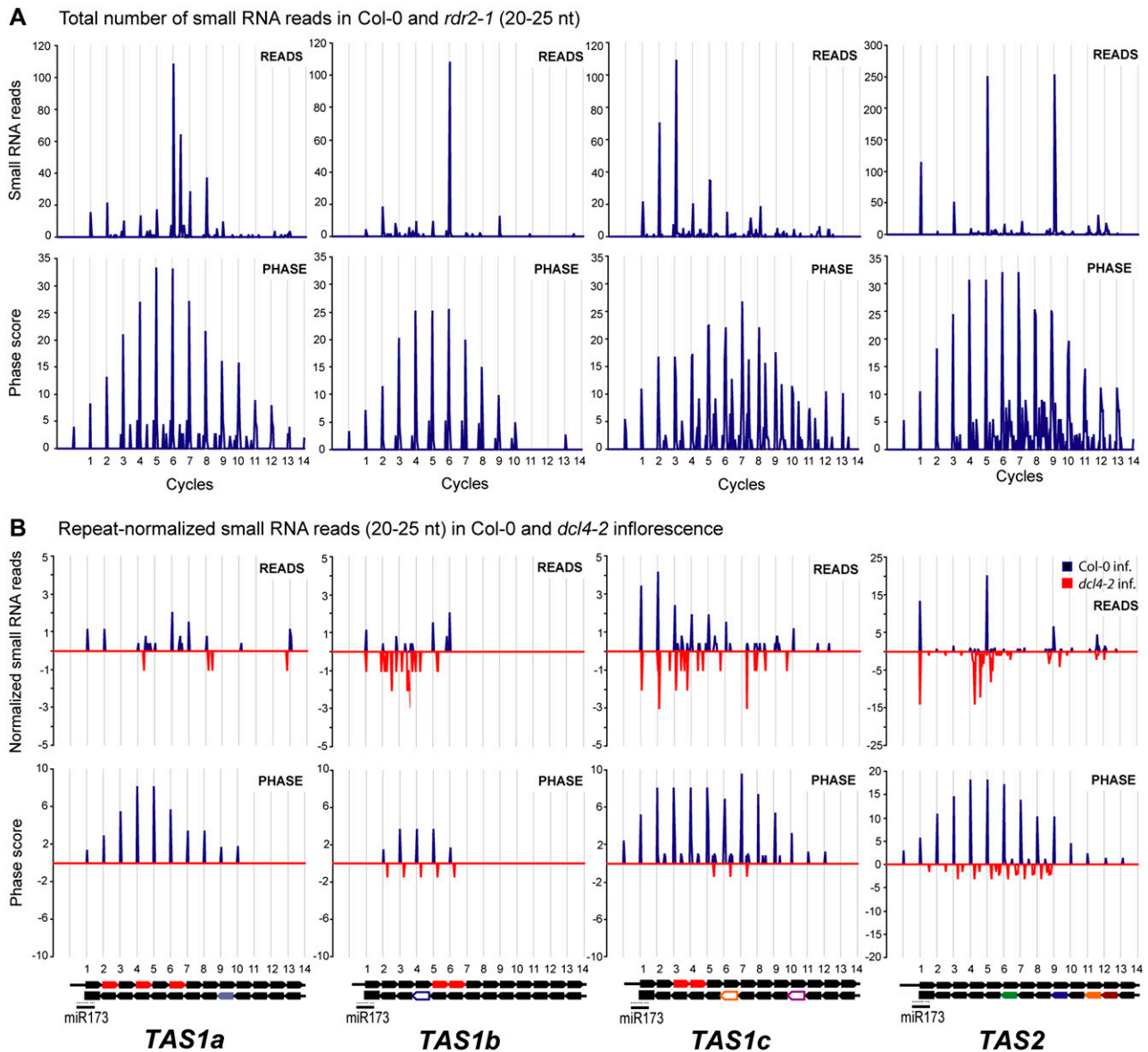


Figure 1. Distribution and Abundance of 21-Nucleotide Small RNAs in *TAS1a*, *TAS1b*, *TAS1c*, and *TAS2*.

(A) Abundance of Col-0 and *rd2-1* small RNA reads in *TAS1a*, *TAS1b*, *TAS1c*, and *TAS2* loci. The top graphs represent the total number of small RNA reads, whereas the bottom graphs show phase signals from Col-0 and *rd2-1* small RNA reads. Gridlines correspond to 21-nucleotide cycles of small RNAs from the miR173-guided cleavage site. nt, nucleotides.

(B) Comparison of Col-0 and *dcl4-2* inflorescence small RNAs. The top graphs represent 20- to 25-nucleotide small RNAs in Col-0 inflorescence versus 20- to 25-nucleotide small RNAs in *dcl4-2* inflorescence for *TAS1a*, *TAS1b*, *TAS1c*, and *TAS2* loci. The bottom graphs show phase signals from Col-0 inflorescence small RNA reads versus *dcl4-2* inflorescence small RNA reads. Small RNA counts were normalized to the size of the *dcl4-2* library and also repeat normalized to account for redundant small RNAs in each locus. The schematics below the phase plots represent miR173-guided cleavage and 21-nucleotide small RNA positions in *TAS1a*, *TAS1b*, *TAS1c*, and *TAS2* transcripts. The position of the miR173 target site is shown as a thin gray line. Thick black arrows represent 21-nucleotide phase positions from the miR173-guided cleavage site. Colored arrows indicate small RNAs previously validated to target various transcripts. White arrows with colored outlines indicate small RNAs with a predicted target. Arrows with identical colors (solid and outlined) indicate small RNAs within the same family. Red arrows indicate small RNA positions for the ASRP255-like family.

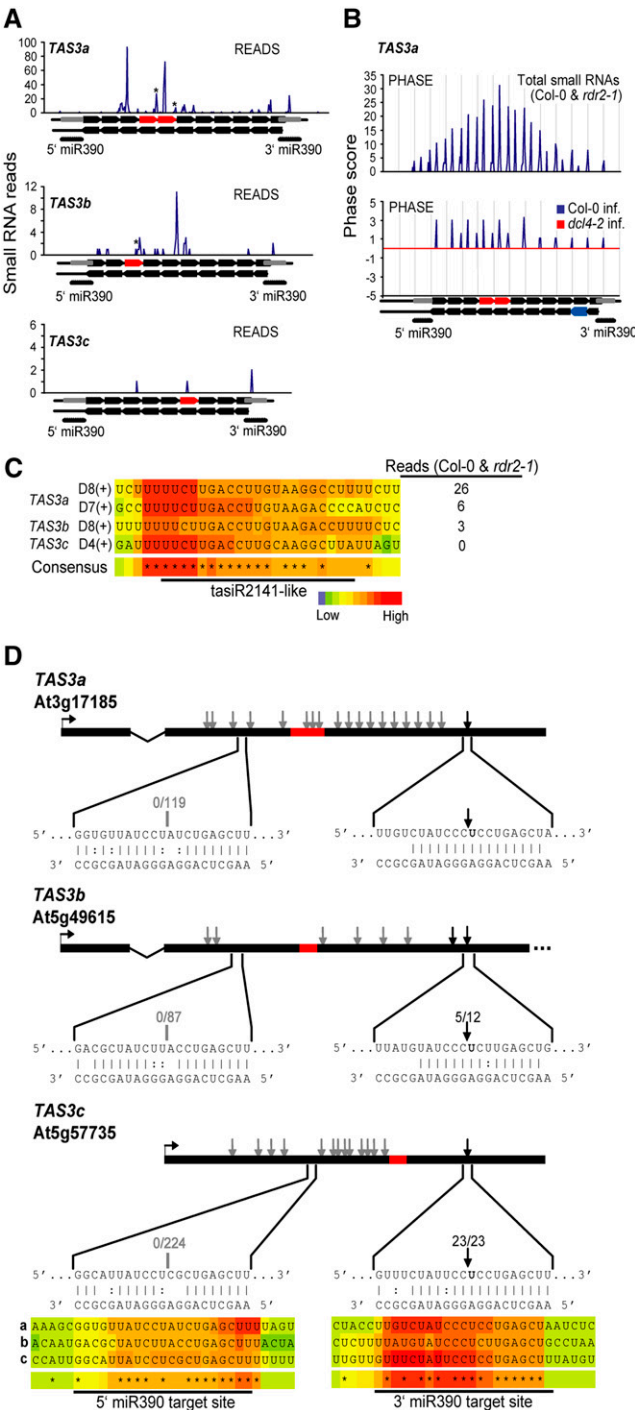


Figure 2. Identification of New Loci and miR390 Target Sites in the *TAS3* Family.

(A) The total number of small RNA reads in Col-0 and *rdr2-1* libraries for *TAS3a* and *TAS3b* and all libraries for *TAS3c* are shown. The 21-nucleotide cycle positions from the 3' miR390-guided cleavage site for each locus are indicated below each graph. Predicted and validated miR390 target sequences are indicated by gray boxes, and ASRP2141-like sequences are indicated by red arrows. Asterisks indicate ASRP2141-like sequences.

that were offset by two nucleotides, with the overhang at the 3' ends, were combined. This accounted for the possibility that either sense or antisense small RNA from a given small RNA duplex might accumulate. Second, a phase score, *P*, was calculated using the following formula:

$$P = \ln \left[\left(1 + \sum_{i=1}^8 k_i \right)^{n-2} \right], P > 0,$$

in which *n* = number of phase cycle positions occupied by at least one small RNA read within an eight-cycle window, and *k* = the total number of reads for all small RNAs with consolidated start coordinates in a given phase within an eight-cycle window. Phase cycle length was set at 21 nucleotides. A positive phase signal, therefore, was limited by the power function (*n* – 2) to those loci with small RNAs occupying at least three cycle positions in a phased, 21-nucleotide register. Requiring occupation of three positions in an eight-cycle window limited the possibility of a positive phase score by chance. It should also be noted that the phase score amplitude is influenced by both small RNA abundance and number of positions occupied. This calculation was applied in a scrolling window format with single nucleotide advances, and scores were assigned to the fourth cycle position in phasing plots (Figure 1).

Small RNAs were detected unidirectionally downstream of the miR173-guided cleavage site from each *TAS1* and *TAS2* locus (Figure 1A; <http://asrp.cgrb.oregonstate.edu/db/>). Phase plots clearly revealed the dominant phasing event to be coincident with the miR173 target site for each locus, although both the raw read and phase transform plots revealed out-of-phase noise at each locus. Phase drift was detected at *TAS1c*, with small RNAs accumulating in the phase position one nucleotide forward from the initial miR173-directed phase, starting at cycle five (Figure 1A). Between cycles 1 and 5, the phase-forward:initial phase ratio of small RNA reads at *TAS1c* was 1:5; however, between cycles 6 and 10, the phase-forward:initial phase ratio at *TAS1c* was 22:1. For *TAS3a*, small RNAs were detected exclusively upstream of the 3' miR390 target site (Figure 2A). The miR390-initiated phase

(B) Phase plots for *TAS3a* tasiRNAs from Col-0 and *rdr2-1* (top) and from normalized reads from Col-0 (bottom, above the x axis) or *dcl4-2* (bottom, below the x axis). Vertical gridlines indicate 21-nucleotide cycles.

(C) T-Coffee alignment of ASRP2141-like sequences from *TAS3a*, *TAS3b*, and *TAS3c*. Identical positions are indicated by asterisks in the consensus plot. The numbers of ASRP2141-like tasiRNA reads in Col-0 and *rdr2-1* libraries are listed.

(D) Diagrammatic representation of primary *TAS3* transcripts and validation of 3' miR390 cleavage sites by 5' RACE. ASRP2141-like regions are highlighted in red. The miR390 and target mRNA duplexes are shown in the expanded regions. Bases in bold indicate predicted cleavage sites. Arrowheads indicate positions corresponding to the 5' end of at least one cloned 5' RACE PCR product. The 5' RACE products sequenced for each miR390 target site are indicated in gray and black, respectively. The number of specific 5' RACE products/total products sequenced at each miR390 target site is indicated. The 3' miR390 target site for *TAS3a* was reported by Allen et al. (2005). T-Coffee alignment of 5' and 3' miR390 target sites in *TAS3a* (a), *TAS3b* (b), and *TAS3c* (c). Identical positions are indicated by asterisks in the consensus plot.

signal, however, was slightly lower than an out-of-phase signal, which likely originated from a secondary targeting event guided by an siRNA from the 5'D2(–) position (Figure 2B; Allen et al., 2005; Axtell et al., 2006). Accurately phased, miR390-initiated RNAs were detected close to the 3' target site at *TAS3a*, but phase-forward drift was detected after several cycles (Figure 2). Between cycles 1 and 6, the phase-forward:initial phase ratio of small RNA reads at *TAS3a* was 1:3. However, the phase-forward:initial phase ratio was 32:1 at cycles 7 and 8. This may be an adapted feature of *TAS3a*, as the functional tasiRNAs occur in the forward phase at the 5'D7(+) and 5'D8(+) positions (positional nomenclature from Allen et al. [2005]).

The basis for phase-forward drift at *TAS3a* and *TAS1c* could be due, at least in part, to non-21-nucleotide siRNAs resulting from misprocessing by DCL4 or alternate DCLs. Alternate-size small RNAs were detected at relatively low levels for most *TAS* loci, although an abundant 22-nucleotide RNA from *TAS1c* was detected at the fifth processing cycle from the miR173 target site (<http://asrp.cgrb.oregonstate.edu/db/>). Loss of DCL4 in the *dcl4-2* mutant resulted in off-sized RNAs at each *TAS* locus (Table 2, Figure 1B). Although the abundance of total small RNAs arising from *TAS1*, *TAS2*, and *TAS3* loci was only modestly affected, the ratio of 21-nucleotide to non-21-nucleotide RNAs was considerably lower in the mutant (Table 2). Importantly, this was accompanied by loss of miRNA-guided phasing (Figures 1B and 2B), and loss of functional tasiRNAs, at each locus. Therefore, although DCL4 is not required to process dsRNA formed from each *TAS* locus, it is clearly necessary for biogenesis of active, properly phased tasiRNAs.

A search for previously unrecognized members of *TAS1*, *TAS2*, and *TAS3* families revealed two additional *TAS3* family members (*TAS3b* and *TAS3c*), which contained sequences similar to *ARF3*- and *ARF4*-targeting tasiR2141 from the originally characterized *TAS3a* locus (Figure 2C). *TAS3b* was previously identified as a tasiRNA-like region by Lu et al. (2006). Unlike *TAS3a*, both *TAS3b* and *TAS3c* contain only a single tasiR2141-like sequence. RDR6-dependent small RNAs of predominantly 21 nucleotides were detected from both *TAS3b* and *TAS3c* (Table 2; <http://asrp.cgrb.oregonstate.edu/db/>), although *TAS3c* generated relatively few RNAs. Importantly, nucleotide sequence alignments and target validation assays revealed a functional miR390-guided cleavage site on the 3' side of both *TAS3b* and *TAS3c* tasiRNA-generating regions (Figure 2D). The tasiR2141-like sequence was detected in the miR390-initiated phase for *TAS3c*, but in the +4 forward phase for *TAS3b*. Transcripts for each *TAS3* locus were detected, and 5' transcription start sites were mapped (see Supplemental Figure 1 online). Therefore, *TAS3* tasiRNAs arise from a small multigene family, all members of which have conserved miR390-guided target sites.

Interestingly, in addition to the conserved 3' miR390 target sites and tasiR2141-related sequences, conserved miR390 target sites on the 5' side of *TAS3a*, *TAS3b*, and *TAS3c* tasiRNA-generating sequences were detected (Figure 2D). In each case, however, the site deviates from canonical plant miRNA target sites in that mispairs and G:U pairs occur at positions 9 to 11 (relative to the 5' end of miR390; Figure 2D). Based on mutational and informatic analyses of naturally occurring target sites, mispairs and G:U pairs at these positions were predicted to have restricted miR390-

guided cleavage (Jones-Rhoades and Bartel, 2004; Mallory et al., 2004; Allen et al., 2005; Schwab et al., 2005). Indeed, 5' rapid amplification of cDNA ends (RACE) analysis failed to detect any cleavage products corresponding to an active 5' miR390 target site, although 5' RACE products were detected at low frequencies at several sites flanking the noncanonical target site at each locus (Figure 2D). Given the high degree of conservation, we conclude that the site is likely important, but functional in a mode that does not depend on target cleavage. Axtell et al. (2006) also detected the noncanonical 5' miR390 site in *TAS3a* and showed that it functions in a noncleavage mode in vivo for *TAS3*-derived tasiRNA biogenesis and function.

Genome-Wide Scans for tasiRNA-Like Loci

To identify loci with tasiRNA-like features or that spawn RDR6/DCL4-dependent siRNAs, a genome-wide scan using Columbia (Col-0) and mutant small RNA sequence libraries was done. These loci were predicted to yield RDR6-dependent, 21-nucleotide RNAs in phased arrays. A set of filters to identify clusters of 21-nucleotide small RNAs that were present in either Col-0 and/or *rdr2-1* mutant libraries, and absent in *rdr6-15* mutant libraries, yielded overlapping sets of 50 and 46 loci in scans of genomic and transcript sequences, respectively (Figure 3; see

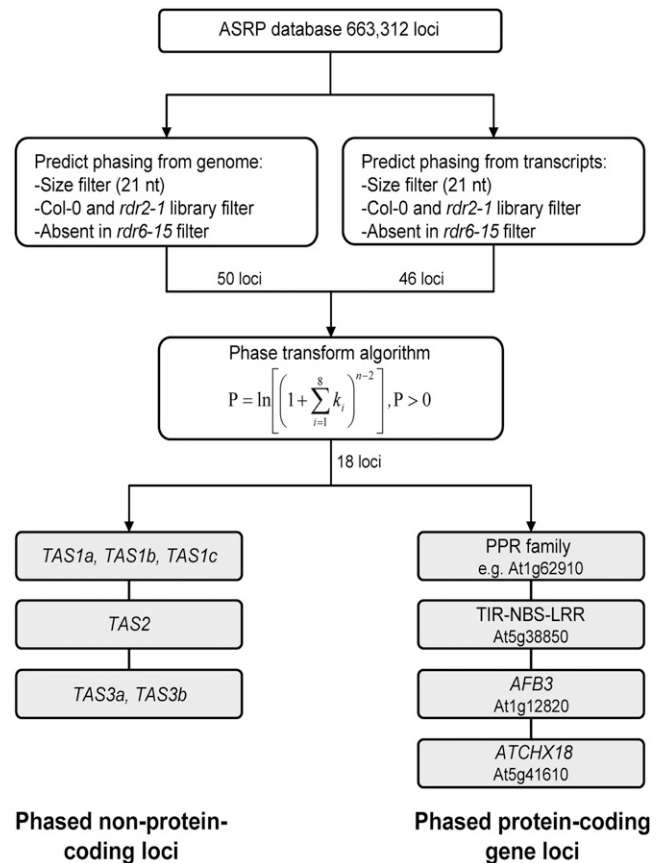


Figure 3. Flowchart for Identification of RDR6-Dependent, Phased, Small RNA-Generating Loci.

Supplemental Table 1 online). Thirty-six of these loci were known to be targeted by at least one miRNA or tasiRNA (see Supplemental Table 1 online). These included overlapping sets of 30 miRNA targets (including seven known *TAS* loci) and 18 tasiRNA targets. Twenty of the 36 loci contained multiple miRNA or tasiRNA target sites. Therefore, among the 50 RDR6-dependent small RNA clusters identified, 72% arose from miRNA/tasiRNA-targeted transcripts and 40% from multiply targeted transcripts. Small RNAs (21 nucleotides) from these loci were generally lost, or accumulated to low levels, in both the *dcl1-7* and *dcl4-2* mutants (see Supplemental Table 1 online), indicating dependence on both miRNA-based and tasiRNA-like mechanisms.

Eighteen loci, including 17 that were targeted by miRNAs/tasiRNAs, contained at least three in-phase (21-nucleotide cycle) positions occupied by at least one small RNA within an eight-cycle window, yielding peak phase scores ranging from 1.4 to 33.1 (Table 2). Except for the known *TAS1*, *TAS2*, and *TAS3* loci that came through the screen, no other non-protein-coding loci were identified. However, three noncoding loci yielded RDR6-dependent, 21-nucleotide RNAs that were phased using a more permissive algorithm in which signal required occupation of only two out of 12 cycle positions (see Supplemental Table 1 online). Two of these loci (from chromosome 4, between coordinate positions 1472767 and 1476524) were embedded in a region with duplications of ubiquitin-like genes or gene sequences (such as At4g03350; see Supplemental Table 1 online). In fact, both small RNA-generating loci contained extensive, continuous similarity to these genes and appear to have resulted from recent duplication events. The other noncoding locus was identified between oppositely oriented genes At5g27650 and At5g27660 but was represented by too few small RNAs in Col-0 plants to allow a meaningful analysis (see Supplemental Table 1 online). Lu et al. (2006) recently identified two *TAS*-like loci from noncoding regions (Chr1:25282658-25283382 and Chr4:13295428-13296124). These loci were not identified here because small RNAs from both loci were RDR6 independent (<http://asrp.cgrb.oregonstate.edu/db/>). The recently identified *TAS4* locus (Rajagopalan et al., 2006) was not identified due to a lack of sequenced small RNAs.

Four gene families were represented among the 12 protein-coding loci that emerged from the phase scan (Table 2). These included a Toll/Interleukin1 receptor-nucleotide binding site-leucine-rich repeat (TIR-NBS-LRR) disease resistance gene (At5g38850; Meyers et al., 2003), the *TIR1*-like *AFB3* gene encoding an F-box protein involved in auxin signaling (At1g12820; Dharmasiri et al., 2005), a cation/hydrogen antiporter gene *ATCHX18* (At5g41610; Sze et al., 2004), and nine genes encoding closely related PPR proteins (discussed below). Transcripts from *AFB3* and *ATCHX18* were targeted and phase-initiated by miR393 and miR856, respectively. Interestingly, two miRNAs (miR856 and miR780) were shown to target the *ATCHX18* transcript (Fahlgren et al., 2007), but phasing is initiated only at the miR856 site. Although the TIR-NBS-LRR gene generated abundant, highly phased siRNAs, we did not identify a miRNA or tasiRNA that initiates phasing. In addition to the miRNA target transcripts that yielded phased siRNAs, targets for miR168 (*AGO1*), miR472 (several CC-NBS-LRR genes), miR393 (*AFB2*), miR773 (*MET2*-like), and miR172 (*AP2*) yielded RDR6-dependent siRNAs that failed to generate a positive phase score (see

Supplemental Table 1 online). siRNAs from many of these genes were also identified in other analyses (Axtell et al., 2006; Lu et al., 2006; Rajagopalan et al., 2006; Ronemus et al., 2006; see Supplemental Table 1 online).

Targeting of *PPR-P* Gene Transcripts and Formation of Phased siRNAs

By far, the most abundant phased, 21-nucleotide siRNA populations were identified from two clusters of *PPR* genes on chromosome 1 (Table 2). The *Arabidopsis thaliana* genome contains at least 448 *PPR*-related genes, which encode putative RNA binding proteins with repeats of a 35-amino acid motif (Lurin et al., 2004). Some PPR proteins are known to regulate RNA processing, stability, editing, or translation in chloroplasts or mitochondria (Lurin et al., 2004; Cushing et al., 2005; Kotera et al., 2005; Okuda et al., 2006; Shikanai, 2006). The PPR proteins are classified into subfamilies containing only tandem arrays of PPR motifs (*PPR-P*) or containing diversified PPR motifs interspersed with non-PPR domains (Aubourg et al., 2000; Lurin et al., 2004; Rivals et al., 2006). A few *PPR-P* genes from *Raphanus sativus* (*Rfo*), *Zea mays* (*Rf-1*), and *Petunia hybrida* (*Rf*) are known restorers of fertility in lines with cytoplasmic male sterility conferred by certain mitochondrial ATPase alleles (Bentolila et al., 2002; Desloire et al., 2003; Kazama and Toriyama, 2003; Wang et al., 2006; Chase, 2007).

Two regions on chromosome 1 contain 21 *PPR-P* genes and pseudogenes, of which 17 (81%) spawned primarily 21-nucleotide siRNAs (Figure 4A). These were dependent on RDR6, DCL4, and DCL1 but independent of RDR1, RDR2, DCL2, and DCL3 (Figure 4A, Table 2; see Supplemental Table 1 online). Phylogenetic analysis of the entire *PPR-P* subfamily revealed that the siRNA-generating loci belonged to a clade of 28 *PPR-P* genes (hereafter referred to as the *PPR-P* clade) that has undergone relatively recent expansion (see below). Using expression profiling arrays, the steady state levels of 23 of the 28 *PPR-P* clade members in inflorescence tissue was measured in each of the *dcl* and *rdp* mutants, in *hen1*, *hst*, and *hyl1* mutants, and in Col-0 and Landsberg *erecta* (*Ler*) plants. The levels of transcripts for the siRNA-generating *PPR-P* genes were generally elevated in the mutants with miRNA or tasiRNA defects (*dcl1*, *dcl4*, *rdp6*, *hen1*, *hst*, and *hyl1*) but not in mutants with defects in other small RNA classes (*dcl2*, *dcl3*, *rdp1*, and *rdp2*) (Figure 4B). Fifty-three percent of siRNA-generated clade genes were significantly upregulated in at least one mutant involved in miRNA and tasiRNA biogenesis (23-gene set, analysis of variance, false discovery rate = 0.05). These data indicate that a high proportion of genes within the clade not only spawn siRNAs with genetic requirements similar to those of tasiRNAs, but that the *PPR-P* transcripts are repressed by posttranscriptional silencing mechanisms.

Computational analysis and experimental validation assays revealed 11 *Arabidopsis* miRNAs and tasiRNAs with potential or validated function to guide cleavage of *PPR-P* mRNAs (Rhoades et al., 2002; Allen et al., 2004; Sunkar and Zhu, 2004; Yoshikawa et al., 2005). These include both forms of miR161 (miR161.1 and miR161.2), miR400, four tasiRNAs from the *TAS1* family, and four tasiRNAs from the *TAS2* locus (Table 2; see Supplemental Figure 2 online). Remarkably, all of these small RNAs were predicted or validated to target *PPR-P* transcripts predominantly from the

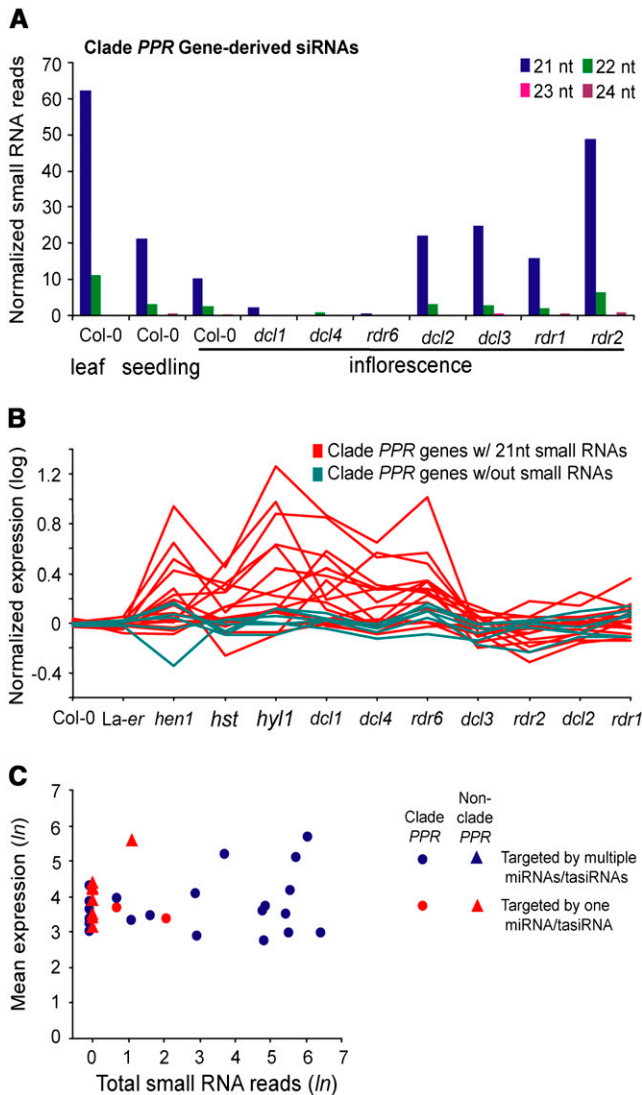


Figure 4. Analysis of *PPR-P* Clade Genes and siRNAs.

(A) Abundance of small RNA size classes from clade *PPR-P* transcripts in various tissues and genotypes.

(B) Expression profile of 23 of the 28 *PPR-P* clade genes in Col-0, Ler, and 10 mutants with defects in silencing factors. Transcripts that yield at least one 21-nucleotide small RNA (red) or no small RNAs (teal) are color-coded. The list of *PPR* genes in the expression profile is as follows: At4g26800, At1g63070, At1g62670, At1g63130, At1g62930, At1g63080, At1g63320, At1g63150, At1g62590, At1g62910, At1g63400, At5g41170, At3g16710, At5g16640, At1g62720, At1g62680, At1g64580, At1g06580, At1g12700, At1g12620, At1g64100, At1g62860, and At1g63630.

(C) Comparison of small RNA reads and expression level of *PPR-P* genes that are targeted by miR161, miR400, and/or tasiRNAs from *TAS1* or *TAS2* loci.

clade, with most clade members targeted by multiple small RNAs (Figure 5A, Table 2; see Supplemental Table 1 online). Five of these genes were validated here by 5' RACE as both miR161 and *TAS2* 3'D6(−) targets (Table 2; see Supplemental Figure 2 online). Combined with previously validated transcript targets (Allen

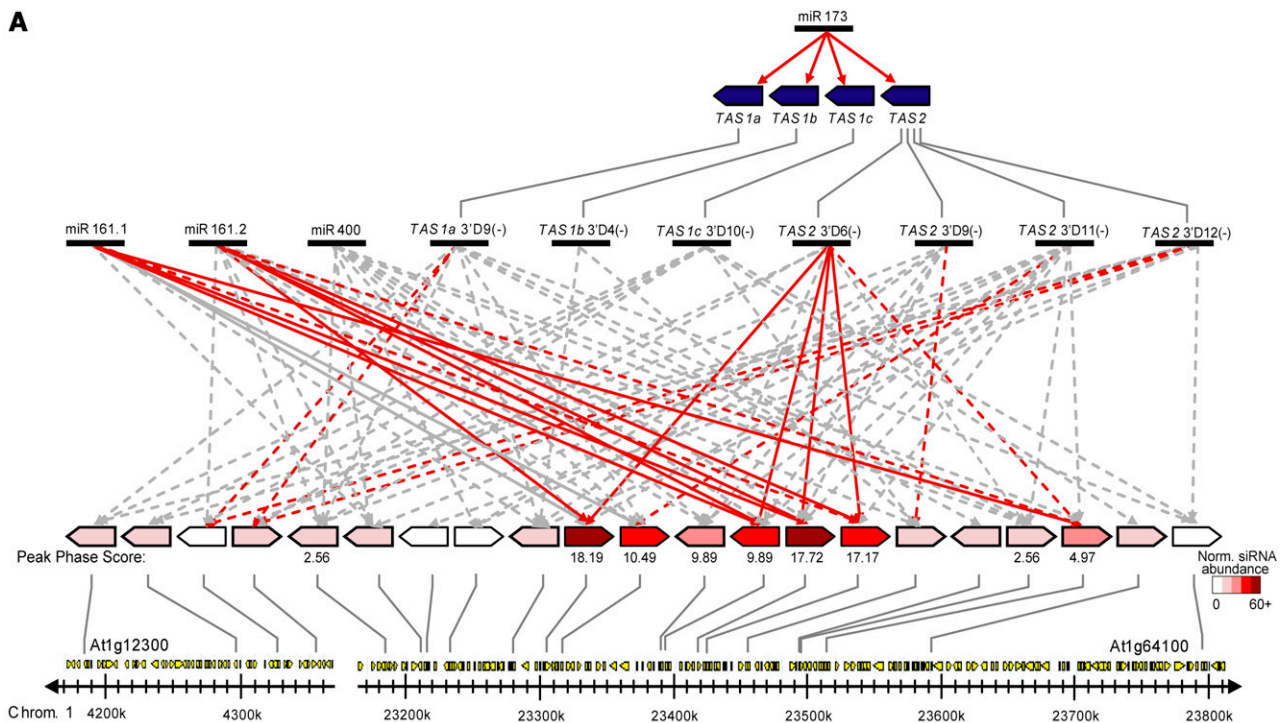
et al., 2004; Yoshikawa et al., 2005), eight *PPR-P* transcripts were validated experimentally as targets for at least one small RNA. As a group, these miRNAs and tasiRNAs were predicted to target a total of 40 *PPR-P* transcripts, including all 28 *PPR* genes in the clade. Although siRNA generation and targeting of clade *PPR-P* transcripts by miRNAs and tasiRNAs were correlated (see below), it was also possible that the high siRNA levels were a reflection of high accumulation levels of the target transcripts. To determine if *PPR* gene-derived siRNA levels were correlated with transcript abundance, the mean expression value in wild-type plants (Col-0 inflorescence tissues) and repeat-normalized siRNA reads were compared. There was no significant correlation between siRNA abundance and transcript level (Pearson correlation coefficient = 0.077; Figure 4C), suggesting that siRNA abundance was related to miRNA and/or tasiRNA targeting rather than to transcript level.

Eight of the nine *PPR-P* genes identified in the genome-wide phase scan contained phase initiation sites corresponding to miR161.1, miR161.2, or *TAS2* 3'D6(−) (Table 2, Figure 6). In fact, loci spawning the highest numbers of siRNAs appeared to correspond to genes with transcripts that were dual-targeted by both miR161 forms and *TAS2* 3'D6(−) (Table 2). In the case of At1g62910, which contains a duplicated coding region resulting in nearly twice as many PPR domains as most other clade proteins, two sets of miR161 and *TAS2* 3'D6(−) target sites and phased siRNAs were identified (Figure 6). None of the other phase patterns from the *PPR-P* sequences were coincident with any other predicted or validated small RNA-guided target sites, although target sites downstream of miR400 were not tested in 5' RACE assays. Curiously, although miR400 was predicted to interact with all but one *PPR* transcript yielding phased siRNAs, no phased RNAs were detected in the vicinity of the miR400 target sites. In fact, each of five *PPR* sequences tested were negative in miR400 target validation assays, even though each miR161 and *TAS2* 3'D6(−) target site tested from the same genes was positive (see Supplemental Figure 2 online). miR400 target validation assays were only done using Col-0 inflorescence tissue, and it is possible that miR400-guided cleavage occurs in other tissues or under different conditions than those tested here.

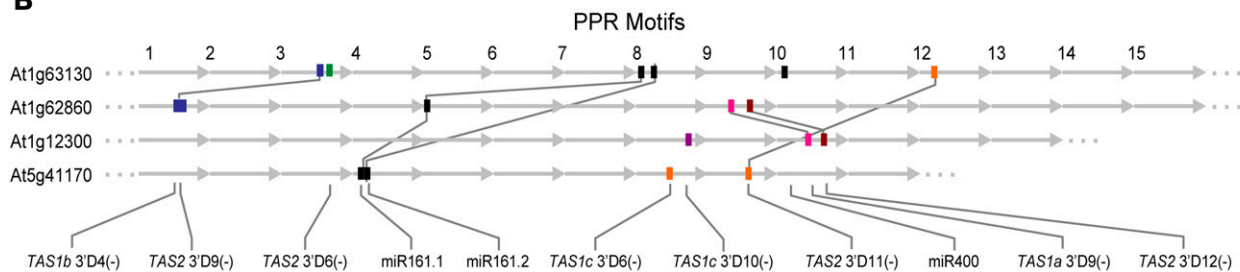
The phasing patterns from miR161 and *TAS2* 3'D6(−) target sites were distinctive. Phased siRNAs from the *TAS2* 3'D6(−) target site generally occurred at the 3' side (Figure 6); indeed, nearly all small RNAs (phased and nonphased) from the targeted *PPR-P* genes occurred at the 3' side of the *TAS2* 3'D6(−) target site, much like tasiRNAs that originate from the 3' side of the miR173-guided cleavage site in *TAS1* and *TAS2* transcripts (Figure 1). By contrast, nearly all of the phased siRNAs initiated at the miR161.1 and miR161.2 target sites occurred on the 5' side of the initiation sites (Figure 6), which is reminiscent of tasiRNAs originating from the 5' side of the miR390-guided cleavage site at *TAS3* loci (Figure 2).

The distribution of predicted or validated target sites for the 11 miRNAs or tasiRNAs within the *Arabidopsis* *PPR-P* clade sequences was analyzed. The miR161.1/miR161.2 and miR400 target sites were separated by several hundred nucleotides in their common target transcripts (Figure 5B). However, in alignments of individual PPR domain-coding regions, it was clear that miR161 and miR400 target sequences span domain-homologous

A



B



C

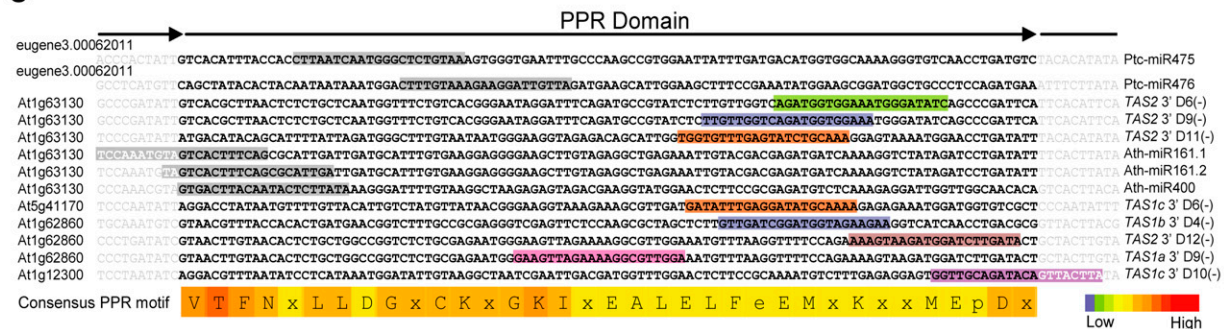


Figure 5. Targeting of the *PPR* Gene Family by miRNAs and tasiRNAs.

miR161.1, miR161.2, miR400, and tasiRNAs from *TAS1* and *TAS2* are predicted to target several *PPR-P* clade transcripts from two gene clusters in chromosome 1.

(A) A schematic representation of *PPR* targeting by miR161.1, miR161.2, miR400, *TAS1a* 3'D9(-) (also named *TAS1a* siR9 by Yoshikawa et al. [2005]), *TAS1b* 3'D4(-) (siR4), *TAS1c* 3'D10(-) (siR10), and *TAS2* 3'D6(-), 3'D9(-), 3'D11(-), and 3'D12(-) (siR6, siR9, siR11, and siR12). Red and gray arrows indicate experimentally validated and predicted-only targets, respectively. Solid arrows indicate targeting events that direct phasing of small RNAs from the *PPR-P* transcript. The peak P score is listed under each gene with phased small RNAs. *PPR* genes are color-coded based on repeat normalized

sequences (Figure 5C). In alignments of miR161 and miR400 foldback sequences, a modest similarity was detected (ClustalW score = 67), raising the possibility that their respective *MIRNA* genes share a common origin. The *TAS1* and *TAS2* tasiRNAs targeted sequences within *PPR* domain 3' coding sequences, which were generally more diverse than the domain 5' regions (Figure 5C). Although some target sequences overlap domain-homologous regions, the tasiRNA target sites represent positions across 65 nucleotides of domain sequence space (Figure 5C). This comparison suggests that targeting of *PPR* transcripts by miRNAs and tasiRNAs likely originated independently on multiple occasions. Interestingly, two *Populus* miRNAs (miR475 and miR476) also have target sites within *PPR* protein-coding transcripts (Lu et al., 2005). These miRNAs target *PPR* domain-coding sequences that are spatially distinct from the *Arabidopsis* small RNA target sites, again suggesting independent origination of *PPR* transcript targeting by distinct small RNAs.

Secondary Targeting of *PPR-P* Gene Transcripts

Prolific generation and amplification of RDR6/DCL4-dependent siRNAs after initial targeting by miRNAs and tasiRNAs could potentially reinforce silencing of *PPR-P* clade transcripts. They could also potentially trigger a cascade of reactions in which silencing spreads through the *PPR* gene family. To assess the potential of secondary targeting by siRNAs from the 28-member *PPR-P* clade, genome-wide targets were computationally predicted for antisense 21-nucleotide small RNAs arising from clade sequences. Targets were predicted based on the same methods used to predict miRNA targets (Figure 7A; Allen et al., 2005; Fahlgren et al., 2007). Secondary siRNA targets were grouped by target score and by their identity as members of the clade, nonclade *PPR-P* genes, or non-*PPR* genes. Hits resulting from perfect complementarity between siRNA and *PPR* gene transcripts (target score = 0) were eliminated, as these could not be assessed in terms of potential targeting in trans. Clade *PPR*-derived siRNAs were more likely to target members of the clade, regardless of their predicted target score (Figures 7B and 7C). The number of nonclade *PPR* and non-*PPR* hits by clade-derived siRNAs increased at higher target score levels (2.5 to 4.0; Figure 7B), as expected for increasing the allowance for mismatches and G:U pairs. This was similar to that observed for miRNA target predictions, where off-target hits were detected at higher scores using both authentic miRNAs and sequence-shuffled miRNAs (Figure 7A). The percentage of non-clade *PPR* hits, however, was

much greater than the percentage of non-*PPR* hits (Figure 7C), suggesting a greater likelihood of clade-derived siRNAs interacting with other *PPR* transcripts rather than non-*PPR* transcripts. Whereas all *PPR-P* clade members, except for one, were potential targets of multiple clade-derived siRNAs, only 72 of the 255 *PPR-P* subfamily members were predicted as targets of at least one siRNA. Thirty-three nonclade *PPR-P* transcripts were predicted targets for two or more clade-derived siRNAs (Figure 7D). Most of these had predicted target scores of 3.5 to 4.0 (Figures 7B and 7C).

Does targeting of siRNAs from clade transcripts lead to amplification of secondary siRNAs from nonclade members? In total, 25 nonclade *PPR-P* loci (11%) yielded at least one siRNA. This is actually below the genome-wide level of protein-coding genes with identity to at least one small RNA (18.2%; Kasschau et al., 2007). Among the 72 and 33 nonclade *PPR-P* transcripts that were plausible predicted targets of at least one or two clade-derived siRNAs, respectively, only nine (12.5%) and six (18.2%) yielded siRNAs. Neither of these percentages were significantly different ($P > 0.27$) from the genome-wide percentage. Additionally, four of these nonclade *PPR-P* small RNA-generating loci (At1g43980, At4g17910, At3g60960, and At5g27300) overlapped with transposons or retroelements and produced predominantly 23- to 24-nucleotide small RNAs (Figure 7D), a feature associated with RDR2/DCL3-dependent siRNAs. Furthermore, there was no correlation between siRNA generation from nonclade *PPR-P* loci and predicted targeting by any of miR161, miR400, or *TAS1* or *TAS2* tasiRNAs (Figure 7D; data not shown). These results argue against secondary targeting by clade-derived siRNAs on non-clade target transcripts.

DISCUSSION

TAS Loci and siRNA Phasing

The tasiRNA biogenesis mechanism employs a novel use for miRNAs as site-specific RNA processing factors. Functional tasiRNAs must be in (or very close to) a 21-nucleotide register with the miRNA-guided cleavage site, otherwise the resulting siRNAs would have limited targeting potential (Vazquez et al., 2004b; Allen et al., 2005; Yoshikawa et al., 2005). Importantly, correct phasing also depends on DCL4. Although small RNAs form in the absence of DCL4, due to alternate activities provided by DCL2 and DCL3 (Dunoyer et al., 2005; Gascioli et al., 2005; Xie et al., 2005), phasing is lost in the *dcl4-2* mutant. Given the

Figure 5. (continued).

abundance of small RNAs from Col-0 and *rdr2-1* libraries. The *PPR* gene clusters are shown relative to genomic position on chromosome 1. From left to right, the *PPR-P* genes are as follows: At1g12300, At1g12620, At1g12700, At1g12775, At1g62590, At1g62670, At1g62680, At1g62720, At1g62860, At1g62910, At1g62930, At1g63070, At1g63080, At1g63130, At1g63150, At1g63230, At1g63320, At1g63330, At1g63400, At1g63630, and At1g64100. **(B)** Schematic representation of *PPR* motifs within four *PPR-P* genes and the location of small RNA target sites relative to the four genes illustrated that they collectively contain targets for all 11 *PPR*-targeting miRNAs and tasiRNAs. Numbers above the diagram indicate the *PPR* motif. Identical colors for miRNA or tasiRNA target sites represent members of the same family. **(C)** *PPR* domain conservation within four *Arabidopsis* *PPR* genes and one *Populus* *PPR* gene. *PPR* domains listed are those that collectively contain target sites for all 11 miRNA or tasiRNA predicted targets from *Arabidopsis* and two known miRNA target sites from *Populus*. Each *PPR* domain consists of 105 nucleotides. Colored boxes indicate the position of the target sites within each *PPR* gene and correspond to colors in **(B)**. A consensus *PPR* motif, with conservation highlighted by a heat map, is shown.

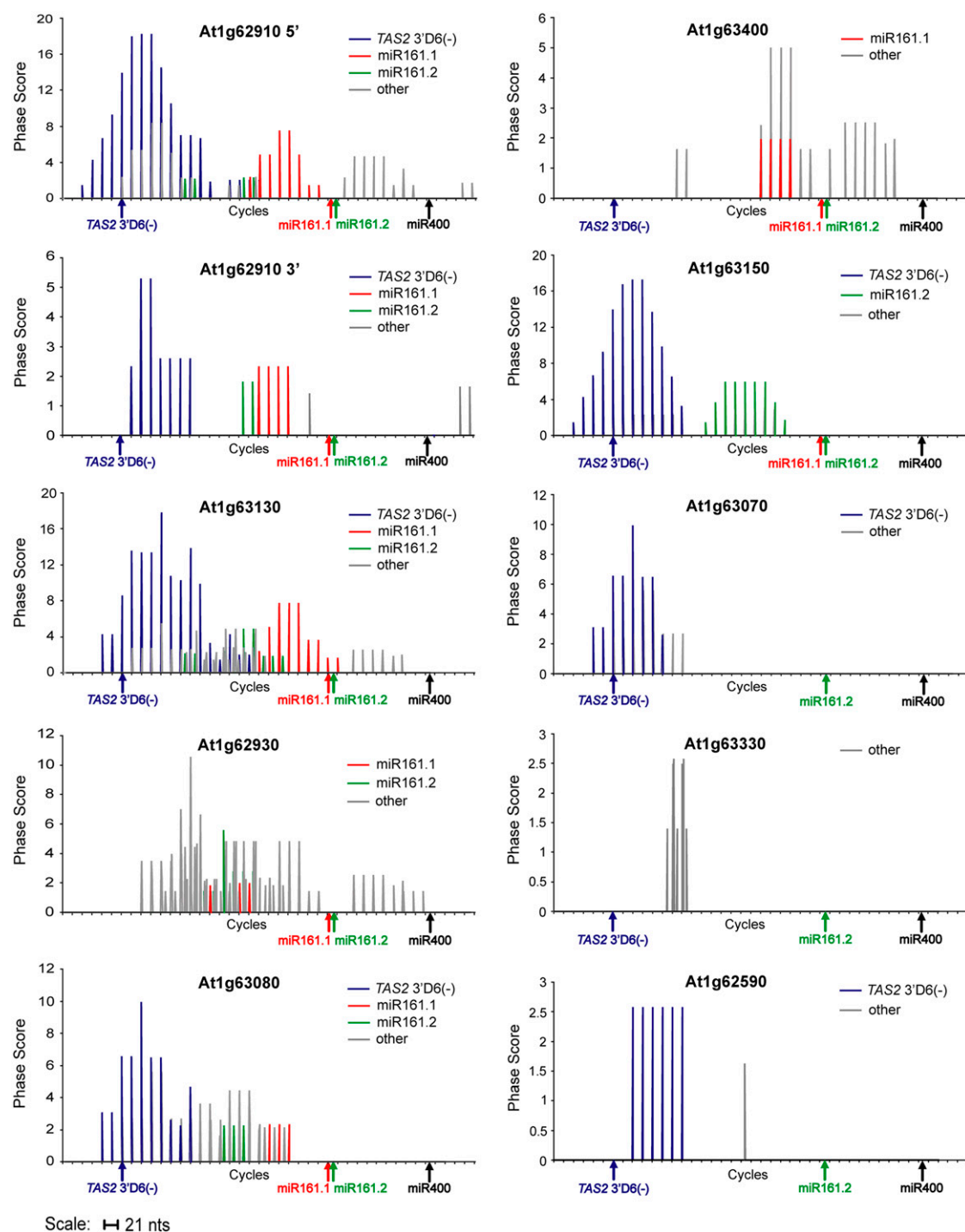


Figure 6. Phase Transform Plots for Nine *Arabidopsis* PPR Genes.

Phased cycles from miR161.1, miR161.2, and TAS2 3'D6(-) target sites are indicated by color coding. Arrows below each plot indicate the miRNA and tasiRNA target sites within each PPR transcript.

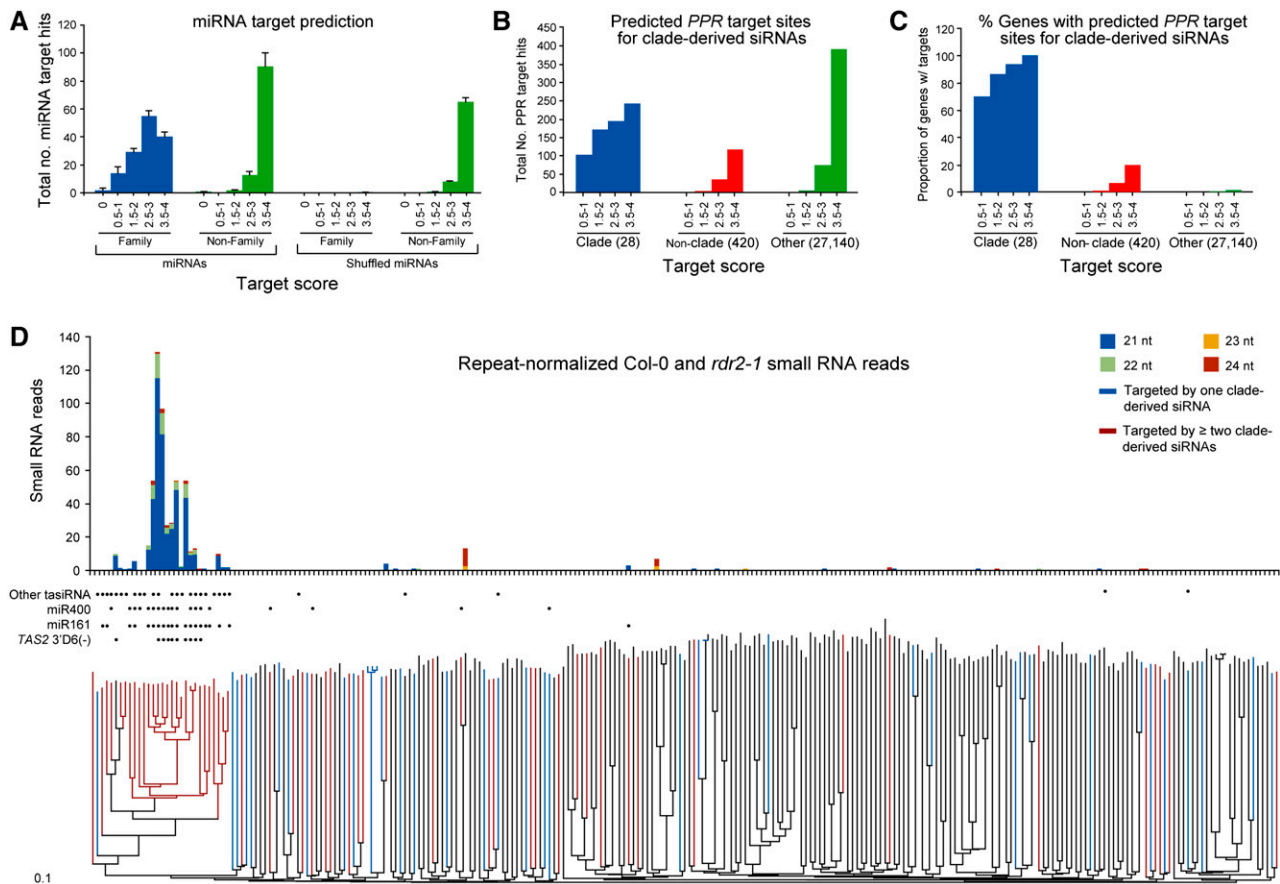


Figure 7. Primary and Secondary Targeting of *PPR-P* Transcripts.

(A) miRNA target prediction for randomly selected miRNA family members (one/family). Target predictions were done with 10 sets of either miRNAs or sequence-shuffled RNAs, and the mean (\pm SD) target score distribution was plotted. miRNA target hits for a validated gene family (blue) or a nonvalidated gene family (green) are grouped according to target score. miRNA families used for target prediction were miR156/157, miR158, miR159/319, miR160, miR161, miR162, miR163, miR164, miR166/165, miR167, miR168, miR169, miR171/170, miR172, miR173, miR390/391, miR393, miR394, miR395, miR396, miR397, miR398, miR399, miR400, miR402, miR403, miR408, miR447, miR773, miR775, miR824, miR827, miR842, miR844, miR856, miR857, and miR858.

(B) Secondary siRNA target prediction for all antisense 21-nucleotide small RNAs arising from all clade *PPR-P* transcripts. Clade-derived siRNAs predicted to target the clade *PPR-P*s (blue), nonclade *PPR*s (red), or non-*PPR*s (green) were plotted by target score. The total number of genes in each group is listed in parenthesis.

(C) The percentage of clade *PPR-P* (blue), nonclade *PPR* (red), and non-*PPR* (green) genes that have transcripts targeted by clade-derived siRNAs. Target hits in **(A)** to **(C)** were grouped according to target score.

(D) Repeat normalized abundance of small RNAs with identity to each *PPR-P* transcript. Dots indicate *PPR-P* transcripts with predicted target sites for miR161, miR400, *TAS2* 3' D6(–), or other tasiRNAs. Transcripts that are singly (blue) or multiply (red) targeted by one or more clade-derived siRNAs are color-coded within the phylogenetic tree. PPR amino acid sequences were aligned using ClustalW with the BLOSUM matrix series. A tree that only differed in the placement of PPR proteins outside of the clade was obtained using the GONNET matrix series (data not shown).

developmental phenotypes and derepression characteristics of tasiRNA target transcripts in *dcl4* mutants, we infer that the off-sized, nonphased small RNAs that originate from *TAS* loci in *dcl4-2* are largely nonfunctional. The structure of DICER from a lower eukaryote indicates that size characteristics of siRNAs are controlled by the spacing between the binding pocket of the PAZ domain, which grips the end of a substrate dsRNA with a 2-nucleotide 3' overhang and the catalytic features at the dual active sites (Macrae et al., 2006). The 21-nucleotide siRNA-generating structure of DCL4, therefore, is a critical property of the enzyme and has been

incorporated as a molecular ruler with physiologic importance. An open question concerns phase drift, which occurs after several DCL4 processing cycles of several tasiRNA precursors. Phase drift occurs at discrete points, such as processing cycle 5 for the *TAS1c* precursor (Figure 1), and may relate to unusual properties of the dsRNA interval interacting with DCL4 at a given cycle.

Two additional *TAS3* loci (*TAS3b* and *TAS3c*) were identified (Figure 2; see Supplemental Table 1 and Supplemental Figure 1 online). These were assigned to the *TAS3* family for two reasons. First, they contained sequenced or predicted tasiRNAs

that were similar to the *ARF3/ARF4* transcript-interacting tasiRNAs from *TAS3a* (Figure 2C; Allen et al., 2005; Williams et al., 2005; Hunter et al., 2006). Second, they contained conserved miR390 target sites on both the 5' and 3' sides of the tasiRNA sequences. Whether or not the *TAS3b* and *TAS3c* tasiRNAs are functional remains to be determined. A mutant carrying a T-DNA insertion in *TAS3a* displayed accelerated phase-change phenotypes similar to those seen in *rdr6* and *dcl4* mutants (Adenot et al., 2006), suggesting that *TAS3b* and *TAS3c* cannot substitute for *TAS3a* function. For each *TAS3* family member, the 3' miR390 target site, but not the 5' target site, was cleaved (Figure 2D). The base pair interactions between miR390 and 5' target sites contain key mismatches that prevent cleavage, and this is a highly conserved and functional feature of the *TAS3* family (Axtell et al., 2006). The consequences of dual targeting of transcripts by miRNAs are discussed in greater detail below.

Genome-Wide Populations of RDR6-Dependent siRNAs

Analysis of the *TAS1*, *TAS2*, and *TAS3* tasiRNA biogenesis and phasing patterns allowed development of an algorithm to detect RDR6-dependent small RNA phase signals from across the *Arabidopsis* genome (Figure 3). Three categories of RDR6-dependent siRNAs were detected (see Supplemental Table 1 online). In the first, tasiRNAs from six *TAS* loci were identified. Neither *TAS3c*, nor the recently recognized *TAS4* (Rajagopalan et al., 2006), loci emerged from the phase scan due to low tasiRNA abundance. Second, three RDR6-dependent loci that were annotated as protein noncoding were identified, although none of these yielded a strong phase signal. Third, 38 protein-coding gene transcripts were identified as RDR6-dependent, as well as DCL1- and DCL4-dependent, generators of 21-nucleotide siRNAs. Nearly all of these are targets of at least one miRNA and/or tasiRNA, and nearly half were targeted by multiple small RNAs. Twelve of these loci yielded strong phase signals that were initiated by one or more miRNA/tasiRNA-guided cleavage events. The absence of a phase signal from the remaining 26 protein-coding genes may have been due, in part, to relatively low siRNA abundance, with more sequencing reads likely to yield more phase signals. Among the loci with a phase signal, only one (At5g38850, encoding a TIR-NBS-LRR protein) lacked a known miRNA or tasiRNA phase initiator (Table 2). These data reveal the strong linkage between endogenous deployment of the RDR6/DCL4 siRNA biogenesis system and small RNA-guided initiation.

The high proportion of dual-targeted transcripts that yield phased siRNAs through the RDR6/DCL4-dependent pathway strongly supports the two-hit trigger hypothesis proposed by Axtell et al. (2006). How efficiently a transcript gets routed through the RDR6/DCL4 siRNA biogenesis pathway may depend on how many small RNA target sites exist and on at least one of these target sites being cleaved. Small RNA-guided effector complexes may interact with factors, such as SGS3, that stabilize one of the cleavage products (Mourrain et al., 2000; Peragine et al., 2004; Yoshikawa et al., 2005). This would then lead to recruitment of RDR6 to the stabilized RNA fragment for dsRNA synthesis and subsequent DCL4-mediated processing in an end-dependent manner. The features governing which small RNA-guided cleavage fragment is stabilized and converted to dsRNA is not clear.

Perhaps a cleavage product that is associated with another small RNA-AGO effector complex, such as that which associates with the 5' fragment from miR390-guided *TAS3* transcript cleavage products, marks a preferred template. The abundance of small RNA target sites, some of which do not guide cleavage, may be what directs the *PPR* transcripts so effectively through the pathway.

The miRNA and RDR6/DCL4-dependent siRNA systems may have coevolved as a posttranscriptional silencing mechanism to limit the activity of the RDR6/DCL4 system on most endogenous transcripts and RNAs. The need for one, and preference for multiple, small RNA-mediated initiation events may disqualify most cellular RNAs as targets. The preference for multiple targeting events also explains why most single-site miRNA target transcripts, which are the vast majority of plant miRNA targets, do not spawn siRNAs (Axtell et al., 2006). Furthermore, it may explain why viral RNAs and other targets of complex populations of siRNAs effectively amplify silencing signals (Brodersen and Voinnet, 2006).

Targeting of a Rapidly Expanding *PPR-P* Gene Clade

Except for *TAS1* and *TAS2* loci, the rapidly evolving *PPR-P* clade yields the most easily recognizable set of RDR6/DCL4-dependent siRNAs in *Arabidopsis*. Most of the *PPR-P* clade transcripts are targeted by multiple miRNAs and/or tasiRNAs, which efficiently drive the cleavage fragments through the RDR6/DCL4 pathway. This very likely reinforces silencing that might be directed via targeting by miR161, miR400, and *TAS1/TAS2* tasiRNAs. Given the abundance of the resulting clade-derived siRNAs, it is puzzling why siRNA biogenesis does not spread outside of the clade. Despite 33 nonclade *PPR-P* transcripts possessing multiple, plausible target sites for sequenced, clade-derived siRNAs, the RDR6/DCL4 system was not directed to this group of transcripts. It is possible that the target prediction algorithm, which we have used successfully with miRNAs and tasiRNAs (Allen et al., 2005; Fahlgren et al., 2007), did not accurately identify prospective targets for this analysis. It is also possible that clade-derived siRNAs had the potential to trigger silencing of nonclade *PPR-P* transcripts, but they were in cellular concentrations that were too low to function. Functional siRNAs may have also been compartmentalized away from nonclade *PPR-P* target transcripts.

What functions might targeting of the *PPR-P* clade by the RDR6/DCL4-dependent silencing system serve? This is not immediately obvious from genetic analysis, as most of the mutant phenotypes associated with loss of *RDR6* and *DCL4* appear to relate specifically to loss of *TAS3* tasiRNAs (Xie et al., 2005; Adenot et al., 2006; Fahlgren et al., 2006; Garcia et al., 2006; Hunter et al., 2006). Of course, physiologic functions for silencing of the clade may lay beyond those that are revealed in short-term growth and development assays. The *PPR* gene family is widespread and has undergone a dramatic evolutionary expansion in plants (Small and Peeters, 2000; Rivals et al., 2006). An important observation is the close phylogenetic relationship between the radish (*R. sativus*) fertility restorer genes (*PPR-A* and *PPR-B*) and members of the targeted *PPR-P* clade in *Arabidopsis* (see Supplemental Figure 3 online; Desloire et al., 2003). The fertility restorer genes compensate for defects in mitochondrion-encoded ATPase alleles in other species (Kazama and Toriyama, 2003; Wen et al.,

2003; Akagi et al., 2004; Wang et al., 2006), although in *Arabidopsis* there are no known mitochondrion-based cytoplasmic male sterility systems and, therefore, no corresponding fertility restorer functions identified. A group of *Populus PPR-P* genes also shows relatively close phylogenetic relationship to fertility restorer genes based on amino acid sequence similarity (data not shown). Interestingly, these genes have expanded in a clade, similar to what has occurred in *Arabidopsis* (see Supplemental Figure 3 online). Expansion of these *PPR-P* clades in several plant species may reflect mechanisms to diversify alleles for interactions with multiple mitochondrial gene alleles. As the functions of the *PPR-P* genes are not known in *Arabidopsis* or *Populus*, the putative allele interactions may not necessarily relate to fertility or be mitochondrion specific. Remarkably, the *Populus PPR-P* clade members are singly or dually targeted by two miRNAs, miR475 and miR476, indicating that this clade is under posttranscriptional regulation (Lu et al., 2005). While primary targeting of *PPR* transcripts in *Arabidopsis* and *Populus* has occurred independently, it is unclear if *Populus PPR* transcripts also spawn secondary siRNAs. Regardless, silencing of the expanding clades in multiple species may serve a dosage compensation function, especially if gene expansion is providing a reservoir of *PPR-P* alleles to balance infrequently dispersed mitochondrial alleles. Posttranscriptional silencing, as we proposed previously (Allen et al., 2004; Fahlgren et al., 2007), may enable rapid expansion of gene families while minimizing detrimental dosage effects.

Finally, while there is compelling evidence that many *MIRNA* genes had evolutionary origins in duplicated segments of protein-coding genes (Allen et al., 2004; Axtell et al., 2006; Fahlgren et al., 2007), the origins of *TAS* gene loci are not clear. However, in view of targeting of the *PPR-P* clade by miRNA and RDR6/DCL4 systems, and the resulting phased siRNA patterns, we speculate that *TAS* loci may originate from miRNA-targeted protein-coding genes. In fact, the abundant siRNA-generating *PPR-P* loci look very similar to known *TAS* loci, except that most still appear to encode functional proteins. However, one can easily imagine loss of protein-coding potential through genetic drift and/or recombination events, but maintenance of one or more functional siRNA modules in phase with initiator small RNA cleavage sites. A nascent *TAS* locus would be retained if suppression of gene-of-origin family members provided an advantage.

METHODS

Small RNA Libraries

Small RNA libraries were described by Kasschau et al. (2007). Small RNA sequencing for wild-type (Col-0), *dcl1-7*, *dcl2-1*, *dcl3-1*, *dcl4-2*, *rdr1-1*, *rdr2-1*, and *rdr6-15* inflorescence, Col-0 and *rdr6-15* seedlings, and Col-0 leaf tissues was done by picoliter-scale pyrosequencing (454 Life Sciences; Margulies et al., 2005). All small RNA sequences are available for download at the Gene Expression Omnibus (GEO) (Edgar et al., 2002; Barrett et al., 2005; <http://www.ncbi.nlm.nih.gov/geo/>) under accession number GSE6682 and the *Arabidopsis* Small RNA Project Database (<http://asrp.cgrb.oregonstate.edu/db/>).

Arabidopsis thaliana Mutants and Target Validation

Mutant lines for *dcl1-7*, *dcl2-1*, *dcl3-1*, *dcl4-2*, *rdr1-1*, *rdr2-1*, *rdr6-15*, *hen1-1*, *hst-15*, and *hyl1-2* were described previously (Park et al., 2002;

Reinhart et al., 2002; Peragine et al., 2004; Vazquez et al., 2004a; Xie et al., 2004, 2005; Allen et al., 2005). Targets were validated using a 5' RACE assay with the GeneRacer kit (Invitrogen) as described previously (Llave et al., 2002; Kasschau et al., 2003; Allen et al., 2004, 2005). Total RNA was isolated from inflorescence tissue of 28-d-old, stage 1 to 12 flowers of both Col-0 and *hen1-1* plants. RNA was subjected to batch and spin column purification for poly(A)⁺ enrichment with an Oligotex mRNA Midi kit (Qiagen). mRNA was subsequently ligated to the GeneRacer RNA oligo adaptor without further modification. The GeneRacer oligo(dT) primer was used to prime cDNA synthesis via reverse transcription. Two rounds of 5' RACE reactions were performed with two gene-specific primers designed ~200 to 500 nucleotides from the 3' end of the predicted target sites using PCR parameters defined by the GeneRacer kit and an annealing temperature of 65°C. The 5' RACE products were gel purified, TOPO TA cloned (Invitrogen), and sequenced.

Alignments, Phase Transformations, and Expression Profiling

Alignments between *TAS3a*, *TAS3b*, and *TAS3c* were performed using T-Coffee (Notredame et al., 2000). Phase transform data were produced using the following equation:

$$P = \ln \left[\left(1 + \sum_{i=1}^8 k_i \right)^{n-2} \right], P > 0,$$

where n = number of phase cycle positions occupied by at least one small RNA read within an eight-cycle window, and k = the total number of reads for all small RNAs with consolidated start coordinates in a given phase within an eight-cycle window.

Phase cycle length was set at 21 nucleotides (see Figure 3). All microarray data were generated using Affymetrix ATH1 arrays and are available at GEO (Edgar et al., 2002; Barrett et al., 2005; <http://www.ncbi.nlm.nih.gov/geo/>).

Phylogenetic Analysis

PPR amino acid sequences were aligned using ClustalW (Higgins et al., 1996) with either the BLOSUM or the GONNET matrix series and with a gap opening penalty of 10 for both the pairwise and multiple alignments and a gap extension penalty of 0.1 and 0.2 for pairwise and multiple alignments, respectively. Gaps in the multiple alignments, defined as regions with at least five consecutive gap characters in all but one or two sequences, were removed. In addition, the first and last 80 positions of the multiple alignments were deleted manually to restrict the analysis to the most conserved region. Trees were produced with ClustalW using the neighbor-joining method (Saitou and Nei, 1987) and 1000 bootstrap replicates. Trees were viewed and rooted using TREEVIEW (Page, 1996).

Accession Numbers

The cDNA sequence for *TAS3b* was deposited in The Arabidopsis Information Resource database under accession number At5g49615. Sequence data from this article can be found in the EMBL/GenBank data libraries under accession number GSE6682 (GEO small RNA data). Col-0 (control for *dcl1-7*, *rdr6-15*, and *dcl4-2*), *dcl1-7*, *rdr6-15*, and *dcl4-2* were from experiments described by Xie et al. (2005) (GEO accession number GSE3011, samples GSM65929, GSM65930, GSM65931, GSM65932, GSM65933, GSM65934, GSM65935, GSM65936, GSM65937, GSM65938, GSM65939, GSM65940, GSM65941, GSM65942, and GSM65943). Col-0 (control for *hst-15*, *hyl1-2*, *dcl2-1*, *dcl3-1*, *rdr1-1*, and *rdr2-1*), *Ler* (control for *hen1-1*), *hst-15*, *hyl1-2*, *dcl2-1*, *dcl3-1*, *rdr1-1*, and *rdr2-1* were from experiments described previously (Allen et al., 2005) (GEO accession number GSE2473, samples GSM47011, GSM47012, GSM47013, GSM47014, GSM47015, GSM47016, GSM47020, GSM47021, GSM47022, GSM47028,

GSM47029, GSM47030, GSM47031, GSM47032, GSM47033, GSM47034, GSM47035, GSM47036, GSM47037, GSM47038, GSM47039, GSM47040, GSM47041, GSM47042, GSM47043, GSM47044, GSM47045, GSM47046, GSM47047, and GSM47048).

Supplemental Data

The following materials are available in the online version of this article.

Supplemental Figure 1. Mapping of Transcription Start Sites of *TAS3* Family Genes by RNA Ligase-Mediated 5' RACE.

Supplemental Figure 2. Mapping of miR161- and *TAS2* 3'D6(-)-Mediated Cleavage Sites in *PPR* Gene Transcripts by 5' RACE.

Supplemental Figure 3. Phylogenetic Tree of PPR-P Clade Proteins from *Arabidopsis*, PPR-P-Related Proteins from *Populus* and *R. sativus*, and Outgroup PPR proteins CRP1 (*Z. mays*), PET309 (*Saccharomyces cerevisiae*), PTC1 (*Homo sapiens*), and RF1A and RF1B (*Oryza sativa*).

Supplemental Table 1. RDR6-Dependent 21-Nucleotide RNA-Generating Loci.

ACKNOWLEDGMENTS

We thank Heather Sweet and Amy Shatswell for excellent technical assistance, Christine Gustin for assistance with 5' RACE analysis, and Erin McWhorter for media preparation. We thank Mark Dasenko for sequence analysis. We also thank Robert Burton for advice on the phase transform equation. This work was supported by grants from the National Science Foundation 2010 Project (MCB-0618433), the National Institutes of Health (AI43288), and the USDA (2006-35301-17420).

Received January 10, 2007; revised February 28, 2007; accepted March 14, 2007; published March 30, 2007.

REFERENCES

- Adenot, X., Elmayan, T., Lauressergues, D., Boutet, S., Bouche, N., Gasciolli, V., and Vaucheret, H. (2006). DRB4-dependent TAS3 trans-acting siRNAs control leaf morphology through AGO7. *Curr. Biol.* **16**: 927–932.
- Akagi, H., Nakamura, A., Yokozeki-Misono, Y., Inagaki, A., Takahashi, H., Mori, K., and Fujimura, T. (2004). Positional cloning of the rice Rf-1 gene, a restorer of BT-type cytoplasmic male sterility that encodes a mitochondria-targeting PPR protein. *Theor. Appl. Genet.* **108**: 1449–1457.
- Allen, E., Xie, Z., Gustafson, A.M., and Carrington, J.C. (2005). MicroRNA-directed phasing during trans-acting siRNA biogenesis in plants. *Cell* **121**: 207–221.
- Allen, E., Xie, Z., Gustafson, A.M., Sung, G.H., Spatafora, J.W., and Carrington, J.C. (2004). Evolution of microRNA genes by inverted duplication of target gene sequences in *Arabidopsis thaliana*. *Nat. Genet.* **36**: 1282–1290.
- Aravin, A., et al. (2006). A novel class of small RNAs bind to MILI protein in mouse testes. *Nature* **442**: 203–207.
- Aubourg, S., Boudet, N., Kreis, M., and Lecharny, A. (2000). In *Arabidopsis thaliana*, 1% of the genome codes for a novel protein family unique to plants. *Plant Mol. Biol.* **42**: 603–613.
- Axtell, M.J., Jan, C., Rajagopalan, R., and Bartel, D.P. (2006). A two-hit trigger for siRNA biogenesis in plants. *Cell* **127**: 565–577.
- Barrett, T., Suzek, T.O., Troup, D.B., Wilhite, S.E., Ngau, W.C., Ledoux, P., Rudnev, D., Lash, A.E., Fujibuchi, W., and Edgar, R. (2005). NCBI GEO: Mining millions of expression profiles—database and tools. *Nucleic Acids Res.* **33**: D562–D566.
- Baulcombe, D. (2004). RNA silencing in plants. *Nature* **431**: 356–363.
- Bentolila, S., Alfonso, A.A., and Hanson, M.R. (2002). A pentatricopeptide repeat-containing gene restores fertility to cytoplasmic male-sterile plants. *Proc. Natl. Acad. Sci. USA* **99**: 10887–10892.
- Borsani, O., Zhu, J., Verslues, P.E., Sunkar, R., and Zhu, J.K. (2005). Endogenous siRNAs derived from a pair of natural cis-antisense transcripts regulate salt tolerance in *Arabidopsis*. *Cell* **123**: 1279–1291.
- Bouche, N., Lauressergues, D., Gasciolli, V., and Vaucheret, H. (2006). An antagonistic function for *Arabidopsis* DCL2 in development and a new function for DCL4 in generating viral siRNAs. *EMBO J.* **25**: 3347–3356.
- Brodersen, P., and Voinnet, O. (2006). The diversity of RNA silencing pathways in plants. *Trends Genet.* **22**: 268–280.
- Chan, S.W., Zilberman, D., Xie, Z., Johansen, L.K., Carrington, J.C., and Jacobsen, S.E. (2004). RNA silencing genes control de novo DNA methylation. *Science* **303**: 1336.
- Chase, C.D. (2007). Cytoplasmic male sterility: A window to the world of plant mitochondrial-nuclear interactions. *Trends Genet.* **23**: 81–90.
- Cushing, D.A., Forsthoefel, N.R., Gestaut, D.R., and Vernon, D.M. (2005). *Arabidopsis* emb175 and other ppr knockout mutants reveal essential roles for pentatricopeptide repeat (PPR) proteins in plant embryogenesis. *Planta* **221**: 424–436.
- Deleris, A., Gallego-Bartolome, J., Bao, J., Kasschau, K.D., Carrington, J.C., and Voinnet, O. (2006). Hierarchical action and inhibition of plant Dicer-like proteins in antiviral defense. *Science* **313**: 68–71.
- Desloire, S., et al. (2003). Identification of the fertility restoration locus, Rfo, in radish, as a member of the pentatricopeptide-repeat protein family. *EMBO Rep.* **4**: 588–594.
- Dharmasiri, N., Dharmasiri, S., Weijers, D., Lechner, E., Yamada, M., Hobbie, L., Ehrismann, J.S., Jurgens, G., and Estelle, M. (2005). Plant development is regulated by a family of auxin receptor F box proteins. *Dev. Cell* **9**: 109–119.
- Dunoyer, P., Himber, C., and Voinnet, O. (2005). DICER-LIKE 4 is required for RNA interference and produces the 21-nucleotide small interfering RNA component of the plant cell-to-cell silencing signal. *Nat. Genet.* **37**: 1356–1360.
- Edgar, R., Domrachev, M., and Lash, A.E. (2002). Gene Expression Omnibus: NCBI gene expression and hybridization array data repository. *Nucleic Acids Res.* **30**: 207–210.
- Fahlgren, N., Howell, M.D., Kasschau, K.D., Chapman, E.J., Sullivan, C.M., Cumbie, J.S., Givan, S.A., Law, T.F., Grant, S.R., Dangl, J.L., and Carrington, J.C. (2007). High-throughput sequencing of *Arabidopsis* microRNAs: Evidence for frequent birth and death of MIRNA genes. *PLoS ONE* **2**: e219.
- Fahlgren, N., Montgomery, T.A., Howell, M.D., Allen, E., Dvorak, S.K., Alexander, A.L., and Carrington, J.C. (2006). Regulation of AUXIN RESPONSE FACTOR3 by TAS3 ta-siRNA affects developmental timing and patterning in *Arabidopsis*. *Curr. Biol.* **16**: 939–944.
- Fusaro, A.F., Matthew, L., Smith, N.A., Curtin, S.J., Dedic-Hagan, J., Ellacott, G.A., Watson, J.M., Wang, M.B., Brosnan, C., Carroll, B.J., and Waterhouse, P.M. (2006). RNA interference-inducing hairpin RNAs in plants act through the viral defence pathway. *EMBO Rep.* **7**: 1168–1175.
- Garcia, D., Collier, S.A., Byrne, M.E., and Martienssen, R.A. (2006). Specification of leaf polarity in *Arabidopsis* via the trans-acting siRNA pathway. *Curr. Biol.* **16**: 933–938.
- Gasciolli, V., Mallory, A.C., Bartel, D.P., and Vaucheret, H. (2005). Partially redundant functions of *Arabidopsis* DICER-like enzymes and a role for DCL4 in producing trans-acting siRNAs. *Curr. Biol.* **15**: 1494–1500.
- Girard, A., Sachidanandam, R., Hannon, G.J., and Carmell, M.A. (2006). A germline-specific class of small RNAs binds mammalian Piwi proteins. *Nature* **442**: 199–202.

- Grivna, S.T., Beyret, E., Wang, Z., and Lin, H. (2006b). A novel class of small RNAs in mouse spermatogenic cells. *Genes Dev.* **20**: 1709–1714.
- Grivna, S.T., Pyhtila, B., and Lin, H. (2006a). MIWI associates with translational machinery and PIWI-interacting RNAs (piRNAs) in regulating spermatogenesis. *Proc. Natl. Acad. Sci. USA* **103**: 13415–13420.
- Henderson, I.R., Zhang, X., Lu, C., Johnson, L., Meyers, B.C., Green, P.J., and Jacobsen, S.E. (2006). Dissecting *Arabidopsis thaliana* DICER function in small RNA processing, gene silencing and DNA methylation patterning. *Nat. Genet.* **38**: 721–725.
- Herr, A.J., Jensen, M.B., Dalmay, T., and Baulcombe, D.C. (2005). RNA polymerase IV directs silencing of endogenous DNA. *Science* **308**: 118–120.
- Higgins, D.G., Thompson, J.D., and Gibson, T.J. (1996). Using CLUSTAL for multiple sequence alignments. *Methods Enzymol.* **266**: 383–402.
- Hunter, C., Sun, H., and Poethig, R.S. (2003). The *Arabidopsis* heterochronic gene *ZIPPY* is an ARGONAUTE family member. *Curr. Biol.* **13**: 1734–1739.
- Hunter, C., Willmann, M.R., Wu, G., Yoshikawa, M., de la Luz Gutierrez-Nava, M., and Poethig, S.R. (2006). Trans-acting siRNA-mediated repression of ETTIN and ARF4 regulates heteroblasty in *Arabidopsis*. *Development* **133**: 2973–2981.
- Jones-Rhoades, M.W., and Bartel, D.P. (2004). Computational identification of plant microRNAs and their targets, including a stress-induced miRNA. *Mol. Cell* **14**: 787–799.
- Kanno, T., Huettel, B., Mette, M.F., Aufsatz, W., Jaligot, E., Daxinger, L., Kreil, D.P., Matzke, M., and Matzke, A.J. (2005). Atypical RNA polymerase subunits required for RNA-directed DNA methylation. *Nat. Genet.* **37**: 761–765.
- Kasschau, K.D., Fahlgren, N., Chapman, E.J., Sullivan, C.M., Cumbie, J.S., Givan, S.A., and Carrington, J.C. (2007). Genome-wide profiling and analysis of *Arabidopsis* siRNAs. *PLoS Biol.* **5**: e57.
- Kasschau, K.D., Xie, Z., Allen, E., Llave, C., Chapman, E.J., Krizan, K.A., and Carrington, J.C. (2003). P1/HC-Pro, a viral suppressor of RNA silencing, interferes with *Arabidopsis* development and miRNA function. *Dev. Cell* **4**: 205–217.
- Katiyar-Agarwal, S., Morgan, R., Dahlbeck, D., Borsani, O., Villegas, A., Jr., Zhu, J.K., Staskawicz, B.J., and Jin, H. (2006). A pathogen-inducible endogenous siRNA in plant immunity. *Proc. Natl. Acad. Sci. USA* **103**: 18002–18007.
- Kazama, T., and Toriyama, K. (2003). A pentatricopeptide repeat-containing gene that promotes the processing of aberrant atp6 RNA of cytoplasmic male-sterile rice. *FEBS Lett.* **544**: 99–102.
- Kim, V.N. (2006). Small RNAs just got bigger: Piwi-interacting RNAs (piRNAs) in mammalian testes. *Genes Dev.* **20**: 1993–1997.
- Kotera, E., Tasaka, M., and Shikanai, T. (2005). A pentatricopeptide repeat protein is essential for RNA editing in chloroplasts. *Nature* **433**: 326–330.
- Lau, N.C., Seto, A.G., Kim, J., Kuramochi-Miyagawa, S., Nakano, T., Bartel, D.P., and Kingston, R.E. (2006). Characterization of the piRNA complex from rat testes. *Science* **313**: 363–367.
- Llave, C., Xie, Z., Kasschau, K.D., and Carrington, J.C. (2002). Cleavage of Scarecrow-like mRNA targets directed by a class of *Arabidopsis* miRNA. *Science* **297**: 2053–2056.
- Lu, C., Kulkarni, K., Souret, F.F., Muthuvallippan, R., Tej, S.S., Poethig, R.S., Henderson, I.R., Jacobsen, S.E., Wang, W., Green, P.J., and Meyers, B.C. (2006). MicroRNAs and other small RNAs enriched in the *Arabidopsis* RNA-dependent RNA polymerase-2 mutant. *Genome Res.* **16**: 1276–1288.
- Lu, S., Sun, Y.H., Shi, R., Clark, C., Li, L., and Chiang, V.L. (2005). Novel and mechanical stress-responsive microRNAs in *Populus trichocarpa* that are absent from *Arabidopsis*. *Plant Cell* **17**: 2186–2203.
- Lurin, C., et al. (2004). Genome-wide analysis of *Arabidopsis* pentatricopeptide repeat proteins reveals their essential role in organelle biogenesis. *Plant Cell* **16**: 2089–2103.
- Macrae, I.J., Zhou, K., Li, F., Repic, A., Brooks, A.N., Cande, W.Z., Adams, P.D., and Doudna, J.A. (2006). Structural basis for double-stranded RNA processing by Dicer. *Science* **311**: 195–198.
- Mallory, A.C., Reinhart, B.J., Jones-Rhoades, M.W., Tang, G., Zamore, P.D., Barton, M.K., and Bartel, D.P. (2004). MicroRNA control of PHABULOSA in leaf development: importance of pairing to the micro-RNA 5' region. *EMBO J.* **23**: 3356–3364.
- Margulies, M., et al. (2005). Genome sequencing in microfabricated high-density picolitre reactors. *Nature* **437**: 376–380.
- Martienssen, R.A., Zaratiegui, M., and Goto, D.B. (2005). RNA interference and heterochromatin in the fission yeast *Schizosaccharomyces pombe*. *Trends Genet.* **21**: 450–456.
- Mello, C.C., and Conte, D., Jr. (2004). Revealing the world of RNA interference. *Nature* **431**: 338–342.
- Meyers, B.C., Kozik, A., Griego, A., Kuang, H., and Michelmore, R.W. (2003). Genome-wide analysis of NBS-LRR-encoding genes in *Arabidopsis*. *Plant Cell* **15**: 809–834.
- Mourrain, P., et al. (2000). *Arabidopsis* SGS2 and SGS3 genes are required for posttranscriptional gene silencing and natural virus resistance. *Cell* **101**: 533–542.
- Mourrain, P., van Blokland, R., Kooter, J.M., and Vaucheret, H. (2007). A single transgene locus triggers both transcriptional and post-transcriptional silencing through double-stranded RNA production. *Planta* **225**: 365–379.
- Munroe, S.H., and Zhu, J. (2006). Overlapping transcripts, double-stranded RNA and antisense regulation: a genomic perspective. *Cell. Mol. Life Sci.* **63**: 2102–2118.
- Notredame, C., Higgins, D.G., and Heringa, J. (2000). T-Coffee: A novel method for fast and accurate multiple sequence alignment. *J. Mol. Biol.* **302**: 205–217.
- Okuda, K., Nakamura, T., Sugita, M., Shimizu, T., and Shikanai, T. (2006). A pentatricopeptide repeat protein is a site recognition factor in chloroplast RNA editing. *J. Biol. Chem.* **281**: 37661–37667.
- Onodera, Y., Haag, J.R., Ream, T., Nunes, P.C., Pontes, O., and Pikaard, C.S. (2005). Plant nuclear RNA polymerase IV mediates siRNA and DNA methylation-dependent heterochromatin formation. *Cell* **120**: 613–622.
- Page, R.D. (1996). TreeView: An application to display phylogenetic trees on personal computers. *Comput. Appl. Biosci.* **12**: 357–358.
- Park, W., Li, J., Song, R., Messing, J., and Chen, X. (2002). CARPEL FACTORY, a Dicer homolog, and HEN1, a novel protein, act in microRNA metabolism in *Arabidopsis thaliana*. *Curr. Biol.* **12**: 1484–1495.
- Peragine, A., Yoshikawa, M., Wu, G., Albrecht, H.L., and Poethig, R.S. (2004). SGS3 and SGS2/SDE1/RDR6 are required for juvenile development and the production of trans-acting siRNAs in *Arabidopsis*. *Genes Dev.* **18**: 2368–2379.
- Pontier, D., Yahubyan, G., Vega, D., Bulski, A., Saez-Vasquez, J., Hakimi, M.A., Lerbs-Mache, S., Colot, V., and Lagrange, T. (2005). Reinforcement of silencing at transposons and highly repeated sequences requires the concerted action of two distinct RNA polymerases IV in *Arabidopsis*. *Genes Dev.* **19**: 2030–2040.
- Rajagopalan, R., Vaucheret, H., Trejo, J., and Bartel, D.P. (2006). A diverse and evolutionarily fluid set of microRNAs in *Arabidopsis thaliana*. *Genes Dev.* **20**: 3407–3425.
- Reinhart, B.J., Weinstein, E.G., Rhoades, M.W., Bartel, B., and Bartel, D.P. (2002). MicroRNAs in plants. *Genes Dev.* **16**: 1616–1626.
- Rhoades, M.W., Reinhart, B.J., Lim, L.P., Burge, C.B., Bartel, B., and Bartel, D.P. (2002). Prediction of plant microRNA targets. *Cell* **110**: 513–520.
- Rivals, E., Bruyere, C., Toffano-Nioche, C., and Lecharny, A. (2006). Formation of the *Arabidopsis* pentatricopeptide repeat family. *Plant Physiol.* **141**: 825–839.

- Ronemus, M., Vaughn, M.W., and Martienssen, R.A.** (2006). MicroRNA-targeted and small interfering RNA-mediated mRNA degradation is regulated by argonaute, dicer, and RNA-dependent RNA polymerase in *Arabidopsis*. *Plant Cell* **18**: 1559–1574.
- Ruby, J.G., Jan, C., Player, C., Axtell, M.J., Lee, W., Nusbaum, C., Ge, H., and Bartel, D.P.** (2006). Large-scale sequencing reveals 21U-RNAs and additional microRNAs and endogenous siRNAs in *C. elegans*. *Cell* **127**: 1193–1207.
- Saitou, N., and Nei, M.** (1987). The neighbor-joining method: A new method for reconstructing phylogenetic trees. *Mol. Biol. Evol.* **4**: 406–425.
- Schwab, R., Palatnik, J.F., Riester, M., Schommer, C., Schmid, M., and Weigel, D.** (2005). Specific effects of microRNAs on the plant transcriptome. *Dev. Cell* **8**: 517–527.
- Shikanai, T.** (2006). RNA editing in plant organelles: Machinery, physiological function and evolution. *Cell. Mol. Life Sci.* **63**: 698–708.
- Small, I.D., and Peeters, N.** (2000). The PPR motif - A TPR-related motif prevalent in plant organellar proteins. *Trends Biochem. Sci.* **25**: 46–47.
- Sunkar, R., and Zhu, J.K.** (2004). Novel and stress-regulated microRNAs and other small RNAs from *Arabidopsis*. *Plant Cell* **16**: 2001–2019.
- Sze, H., Padmanaban, S., Cellier, F., Honys, D., Cheng, N.H., Bock, K.W., Conejero, G., Li, X., Twell, D., Ward, J.M., and Hirschi, K.D.** (2004). Expression patterns of a novel AtCHX gene family highlight potential roles in osmotic adjustment and K⁺ homeostasis in pollen development. *Plant Physiol.* **136**: 2532–2547.
- Talmor-Neiman, M., Stav, R., Klipcan, L., Buxdorf, K., Baulcombe, D.C., and Arazi, T.** (2006). Identification of trans-acting siRNAs in moss and an RNA-dependent RNA polymerase required for their biogenesis. *Plant J.* **48**: 511–521.
- Tolia, N.H., and Joshua-Tor, L.** (2007). Slicer and the Argonautes. *Nat. Chem. Biol.* **3**: 36–43.
- Tomari, Y., and Zamore, P.D.** (2005). Perspective: Machines for RNAi. *Genes Dev.* **19**: 517–529.
- Tran, R.K., Zilberman, D., de Bustos, C., Ditt, R.F., Henikoff, J.G., Lindroth, A.M., Delrow, J., Boyle, T., Kwong, S., Bryson, T.D., Jacobsen, S.E., and Henikoff, S.** (2005). Chromatin and siRNA pathways cooperate to maintain DNA methylation of small transposable elements in *Arabidopsis*. *Genome Biol.* **6**: R90.
- Vaucheret, H.** (2005). MicroRNA-dependent trans-acting siRNA production. *Sci. STKE* **2005**: pe43.
- Vaucheret, H.** (2006). Post-transcriptional small RNA pathways in plants: Mechanisms and regulations. *Genes Dev.* **20**: 759–771.
- Vazquez, F.** (2006). *Arabidopsis* endogenous small RNAs: Highways and byways. *Trends Plant Sci.* **11**: 460–468.
- Vazquez, F., Gasciolli, V., Crete, P., and Vaucheret, H.** (2004a). The nuclear dsRNA binding protein HYL1 is required for microRNA accumulation and plant development, but not posttranscriptional transgene silencing. *Curr. Biol.* **14**: 346–351.
- Vazquez, F., Vaucheret, H., Rajagopalan, R., Lepers, C., Gasciolli, V., Mallory, A.C., Hilbert, J.L., Bartel, D.P., and Crete, P.** (2004b). Endogenous trans-acting siRNAs regulate the accumulation of *Arabidopsis* mRNAs. *Mol. Cell* **16**: 69–79.
- Wang, X.J., Gaasterland, T., and Chua, N.H.** (2005). Genome-wide prediction and identification of cis-natural antisense transcripts in *Arabidopsis thaliana*. *Genome Biol.* **6**: R30.
- Wang, Z., et al.** (2006). Cytoplasmic male sterility of rice with boro II cytoplasm is caused by a cytotoxic peptide and is restored by two related PPR motif genes via distinct modes of mRNA silencing. *Plant Cell* **18**: 676–687.
- Waterhouse, P.M., and Fusaro, A.F.** (2006). Plant science. Viruses face a double defense by plant small RNAs. *Science* **313**: 54–55.
- Waterhouse, P.M., Wang, M.B., and Lough, T.** (2001). Gene silencing as an adaptive defence against viruses. *Nature* **411**: 834–842.
- Wen, L., Ruesch, K.L., Ortega, V.M., Kamps, T.L., Gabay-Laughnan, S., and Chase, C.D.** (2003). A nuclear restorer-of-fertility mutation disrupts accumulation of mitochondrial ATP synthase subunit alpha in developing pollen of S male-sterile maize. *Genetics* **165**: 771–779.
- Williams, L., Carles, C.C., Osmont, K.S., and Fletcher, J.C.** (2005). A database analysis method identifies an endogenous trans-acting short-interfering RNA that targets the *Arabidopsis* *ARF2*, *ARF3*, and *ARF4* genes. *Proc. Natl. Acad. Sci. USA* **102**: 9703–9708.
- Willmann, M.R., and Poethig, R.S.** (2005). Time to grow up: The temporal role of smallRNAs in plants. *Curr. Opin. Plant Biol.* **8**: 548–552.
- Xie, Z., Allen, E., Wilken, A., and Carrington, J.C.** (2005). DICER-LIKE 4 functions in trans-acting small interfering RNA biogenesis and vegetative phase change in *Arabidopsis thaliana*. *Proc. Natl. Acad. Sci. USA* **102**: 12984–12989.
- Xie, Z., Johansen, L.K., Gustafson, A.M., Kasschau, K.D., Lellis, A.D., Zilberman, D., Jacobsen, S.E., and Carrington, J.C.** (2004). Genetic and functional diversification of small RNA pathways in plants. *PLoS Biol.* **2**: E104.
- Yoshikawa, M., Peragine, A., Park, M.Y., and Poethig, R.S.** (2005). A pathway for the biogenesis of trans-acting siRNAs in *Arabidopsis*. *Genes Dev.* **19**: 2164–2175.
- Zilberman, D., Cao, X., and Jacobsen, S.E.** (2003). ARGONAUTE4 control of locus-specific siRNA accumulation and DNA and histone methylation. *Science* **299**: 716–719.
- Zilberman, D., Cao, X., Johansen, L.K., Xie, Z., Carrington, J.C., and Jacobsen, S.E.** (2004). Role of *Arabidopsis* ARGONAUTE4 in RNA-directed DNA methylation triggered by inverted repeats. *Curr. Biol.* **14**: 1214–1220.

Genome-Wide Analysis of the RNA-DEPENDENT RNA POLYMERASE6/DICER-LIKE4 Pathway in *Arabidopsis* Reveals Dependency on miRNA- and tasiRNA-Directed Targeting

Miya D. Howell, Noah Fahlgren, Elisabeth J. Chapman, Jason S. Cumbie, Christopher M. Sullivan, Scott A. Givan, Kristin D. Kasschau and James C. Carrington
Plant Cell 2007;19;926-942; originally published online March 30, 2007;
DOI 10.1105/tpc.107.050062

This information is current as of February 28, 2013

Supplemental Data	http://www.plantcell.org/content/suppl/2011/04/16/tpc.107.050062.DC1.html
References	This article cites 96 articles, 39 of which can be accessed free at: http://www.plantcell.org/content/19/3/926.full.html#ref-list-1
Permissions	https://www.copyright.com/ccc/openurl.do?sid=pd_hw1532298X&issn=1532298X&WT.mc_id=pd_hw1532298X
eTOCs	Sign up for eTOCs at: http://www.plantcell.org/cgi/alerts/ctmain
CiteTrack Alerts	Sign up for CiteTrack Alerts at: http://www.plantcell.org/cgi/alerts/ctmain
Subscription Information	Subscription Information for <i>The Plant Cell</i> and <i>Plant Physiology</i> is available at: http://www.aspb.org/publications/subscriptions.cfm